bioRxiv preprint doi: https://doi.org/10.1101/2021.06.07.447428; this version posted December 22, 2021. The copyright holder for this preprint (which was not certified by peer review) is the author/funder, who has granted bioRxiv a license to display the preprint in perpetuity. It is made available under aCC-BY-NC-ND 4.0 International license.

DNA damage models phenotypes of β cell senescence in Type 1 Diabetes

Gabriel Brawerman[1,2], Jasmine Pipella[1,2] and Peter J. Thompson[1,2,3]

[1]Department of Physiology and Pathophysiology, Rady Faculty of Health Sciences, University of Manitoba

[2]Children's Hospital Research Institute of Manitoba, 715 McDermot ave, Winnipeg, MB R3E 3P4, Canada

[3]Corresponding author: peter.thompson@umanitoba.ca , Ph. +01-204-975-7787

Objective. Type 1 Diabetes (T1D) is characterized by progressive loss of insulin-producing pancreatic β cells as a result of autoimmune destruction. In addition to β cell death, recent work has shown that subpopulations of β cells acquire dysfunction during T1D. We previously reported that some β cells adopt a senescent fate involving a DNA damage response (DDR) during the pathogenesis of T1D, however, the question of how senescence develops in β cells has not been investigated.

Methods. Here, we tested the hypothesis that unrepaired DNA damage triggers β cell senescence using culture models including the mouse NIT1 β cell line derived from the T1D-susceptible nonobese diabetic (NOD) strain, human donor islets and EndoC β cells. DNA damage was chemically induced using etoposide or bleomycin and cells or islets were analyzed by a combination of molecular assays for senescence phenotypes including Western blotting, qRT-PCR, Luminex assays, flow cytometry and histochemical staining. RNA-seq was carried out to profile global transcriptomic changes in human islets undergoing DDR and senescence. Insulin ELISAs were used

bioRxiv preprint doi: https://doi.org/10.1101/2021.06.07.447428; this version posted December 22, 2021. The copyright holder for this preprint (which was not certified by peer review) is the author/funder, who has granted bioRxiv a license to display the preprint in perpetuity. It is made available under aCC-BY-NC-ND 4.0 International license.

to quantify glucose stimulated insulin secretion from chemically-induced senescent islets and cells in culture.

Results. Sub-lethal DNA damage in NIT1 cells led to several classical hallmarks of senescence including sustained DDR activation, growth arrest, enlarged flattened morphology and a senescence-associated secretory phenotype (SASP) resembling what occurs in primary β cells during T1D in NOD mice. Some of these phenotypes differed between NIT1 cells and the MIN6 β cell line derived from a non-T1D susceptible mouse strain. RNA-seq analysis of human islets undergoing DDR and early senescence revealed a coordinated p53-p21 transcriptional program and upregulation of prosurvival signaling and SASP genes, which were confirmed in independent islet preparations at the protein level. Importantly, chemically induced DNA damage also led to DDR activation and senescence phenotypes in the EndoC-βH5 human β cell line, confirming that this response can occur directly in human β cells. Finally, DNA damage and senescence in both mouse β cell lines and human islets led to decreased insulin content.

Conclusions. Taken together, these findings suggest that some of the phenotypes of β cell senescence during T1D can be modeled by chemically induced DNA damage in mouse β cell lines and human islets and β cells in culture. These culture models will be useful tools to understand some of the mechanisms of β cell senescence in T1D.

Keywords: Pancreatic β cells; Senescence; DNA damage response; Type 1 Diabetes

Highlights:

bioRxiv preprint doi: https://doi.org/10.1101/2021.06.07.447428; this version posted December 22, 2021. The copyright holder for this preprint (which was not certified by peer review) is the author/funder, who has granted bioRxiv a license to display the preprint in perpetuity. It is made available under aCC-BY-NC-ND 4.0 International license.

- DNA damage induces senescent phenotypes in mouse β cell lines
- DNA damage induces a p53-p21 transcriptional program and senescent phenotypes in human islets and EndoC cells
- DNA damage and senescence leads to decreased insulin content
- DNA damage models some aspects of β cell senescence in Type 1 Diabetes

1. Introduction

Type 1 Diabetes (T1D) is a disease of chronic insulin deficiency due to progressive autoimmune-mediated destruction of pancreatic β cells [1]. While much of our understanding of T1D stems from investigations of the immune system, recent work has implicated stress responses in β cells as an additional factor driving disease progression and onset [2,3]. For instance, β cells experience unmitigated endoplasmic reticulum (ER) stress and activate the terminal unfolded protein response (UPR) leading to apoptosis during the development of T1D [4]. Small molecule therapeutics that block terminal UPR have shown promise in clinical trials of new onset T1D patients by slowing the decline in C-peptide production after diagnosis [5,6]. Thus, clinical interventions to target β cell stress responses are emerging as a therapeutic strategy for T1D.

In addition to terminal UPR, it was recently shown that a subpopulation of β cells undergo senescence during the pathogenesis of T1D [7]. Cellular senescence is a complex and dynamic program of irreversible cell cycle arrest, typically initiated as a consequence of aging, oncogene activation, or a variety of stressors, and has many different biological functions including tumor suppression, wound healing, tissue regeneration and embryonic patterning [8,9]. Senescence resulting from unrepairable cell stress or damage is usually activated via a combination of the $p16^{Ink4a}$/Rb and/or p53-p21 pathways, leading to permanent growth arrest and hallmark phenotypes such

bioRxiv preprint doi: https://doi.org/10.1101/2021.06.07.447428; this version posted December 22, 2021. The copyright holder for this preprint (which was not certified by peer review) is the author/funder, who has granted bioRxiv a license to display the preprint in perpetuity. It is made available under aCC-BY-NC-ND 4.0 International license.

as an enlarged cell morphology, senescence-associated βgalactosidase (SA-βgal) activity, persistent DNA damage response (DDR), apoptosis resistance and a senescence-associated secretory phenotype (SASP) [10].

While healthy β cells are progressively destroyed by autoimmunity in T1D, senescent β cells accumulate during the development of T1D in humans and in the preclinical nonobese diabetic (NOD) mouse model for T1D [7]. Senescent β cells in NOD mice are characterized by upregulation of p21 and $p16^{Ink4a}$, DDR activation, a Bcl-2-mediated prosurvival phenotype, elevated SA-βgal activity and a SASP involving IL-6, Igfbp3, Serpine1, Mmp2, and Flnb [7]. The presence of persistent DDR, Bcl-2 upregulation and contents of SASP generally differentiates stress-induced senescence in β cells in T1D from natural aging and β cell senescence in Type 2 Diabetes [11–13]. Notably, in NOD mice, elimination of senescent β cells with Bcl-2 family inhibitors (senolytic compounds), or suppression of SASP with Bromodomain ExtraTerminal domain inhibitors, halts disease progression [7,14]. Therefore, senescence is a novel therapeutic target for T1D prevention.

Despite these advances, basic mechanistic questions around β cell senescence in T1D remain. Senescence progression and phenotypes are variable between cells and are generally cell type- and stress/trigger-dependent [15,16] and although well studied in vitro, are poorly understood in vivo, as there is no one marker that can accurately define senescence in every cell type [17]. However, culture models have been foundational in

bioRxiv preprint doi: https://doi.org/10.1101/2021.06.07.447428; this version posted December 22, 2021. The copyright holder for this preprint (which was not certified by peer review) is the author/funder, who has granted bioRxiv a license to display the preprint in perpetuity. It is made available under aCC-BY-NC-ND 4.0 International license.

defining and characterizing molecular mechanisms and phenotypes. In particular, the specific triggers of β cell senescence in T1D are not known and there is currently no β cell culture model to study the phenomenon. Different inbred mouse strains used to model diabetes have different genetic background polymorphisms that could influence the development of specific senescence phenotypes. For instance, the NOD mouse strain commonly used to model T1D harbors two polymorphisms in the non-homologous end joining repair factor Xrcc4, lowering the efficiency of DNA double-strand break repair in this strain as compared with C57BL strains [18]. Addressing fundamental mechanistic questions around β cell senescence in T1D using mouse models would greatly benefit from a cell line with the relevant genetic background.

As with NOD mice, a subset of β cells in human T1D donors show DDR and activation of the p53-p21 senescence pathway [7,19]. We previously showed that cultured primary adult human islets transcriptionally upregulate p21 (*CDKN1A)* and develop a SASP following induction of DNA double-strand breaks with the chemotherapeutic agent bleomycin [7,14]. These findings suggest that β cell senescence in T1D may involve unrepaired DNA damage, but a comprehensive analysis of the outcomes of DDR induction in human islets has not been performed and it is unclear whether these changes actually occur in β cells, as islets are comprised of a diversity of cell types.

The objectives of this study were to investigate the phenotypes arising in β cells as a result of DDR activation to test the hypothesis that sub-lethal DNA double-strand break

bioRxiv preprint doi: https://doi.org/10.1101/2021.06.07.447428; this version posted December 22, 2021. The copyright holder for this preprint (which was not certified by peer review) is the author/funder, who has granted bioRxiv a license to display the preprint in perpetuity. It is made available under aCC-BY-NC-ND 4.0 International license.

damage triggers senescence in β cells derived from the NOD mouse strain and in human β cells. Our results suggest that chemically triggered DNA damage can be used to accurately model some of the key phenotypes involved in β cell senescence during T1D. We also found that chemically induced DDR and senescence decreases insulin content in mouse β cell lines and human islets. These findings have important implications for culture modeling of β cell senescence and understanding the mechanisms driving senescence in the context of T1D.

2. Materials and Methods.

2.1 Mouse cell line culture and drug treatments.

Mouse insulinoma cell lines MIN6 (RRID:CVCL_0431, sex of cell line is unknown) derived from 13 week C57BL6 mice (gift from Dr. A. Bhushan, UCSF) and NIT1 (RRID: CVCL_3561), derived from 10 week female NOD/LtJ mice (purchased from ATCC) have been previously described [20,21]. Both cell lines were cultured in DMEM high glucose with 2 mM L-glutamine (ThermoFisher) containing 10% FBS (Millipore-Sigma), 20 mM HEPES, 1 mM sodium pyruvate (Gibco), 1X antibiotic-antimycotic (Gibco) and 50 µM 2-mercaptoethanol at 37°C and 5% CO_2. Cell lines were confirmed mycoplasma-free using the PlasmoTest mycoplasma kit (Invivogen). Cell lines were passaged every 4-6 days and MIN6 were detached with 0.25% trypsin-EDTA (Gibco) and seeded at 7.5-1x10^6 cells per 75 cm^2 flask, whereas NIT1 were detached with 0.05% trypsin-EDTA and seeded at 2-2.5x10^6 cells per flask. Cells were used between passages 4 and 25 for all experiments. For senescence induction, we modified a previous method that was

bioRxiv preprint doi: https://doi.org/10.1101/2021.06.07.447428; this version posted December 22, 2021. The copyright holder for this preprint (which was not certified by peer review) is the author/funder, who has granted bioRxiv a license to display the preprint in perpetuity. It is made available under aCC-BY-NC-ND 4.0 International license.

used to trigger "therapy-induced" senescence in mouse melanoma cell line B16-F10 [22]. MIN6 cells were seeded at a density of 0.7-0.85 x 10^5 cells/cm^2 in 12 or 6-well plates, respectively. Twenty-four hours later, normal growth media was replaced with media containing 2 µM etoposide (Millipore-Sigma) or vehicle (0.01% DMSO) for 2 or 3 days, followed by removal of drug by replacing wells with fresh media. Similarly, NIT1 cells were seeded at a density of 0.85-1.15 x 10^5 cells/cm^2 and 24 h later cultured in 0.5 or 0.25 µM etoposide or vehicle (0.0025 or 0.00125% DMSO) for 3 days before drug removal on day 4 as with MIN6 cells. After drug removal, the media was replaced with fresh media every other day. Vehicle-treated cells often reached confluence before drug washout and required passaging prior to drug removal, so cells were passaged into the same concentration of DMSO-containing media and media was replaced at the same time as the etoposide-treated cells. Cell counting and viability assays were performed with trypan blue staining on an automated cell counter (Bio-Rad TC-20). Cells were cultured for indicated times after drug treatment and harvested as indicated for various assays.

2.2 Human islet culture and EndoC-βH5 cells.

Human islets were procured either through the Integrated Islet Distribution Program (IIDP) (for RNA-seq) or from the Alberta Diabetes Institute (ADI). Islets used for RNA-seq were isolated from a healthy nondiabetic female donor of Hispanic ethnicity, age 44 years (RRID:SAMN13186657), from IIDP. Islets from ADI were used for DDR induction and Luminex assays were from a healthy nondiabetic Caucasian male donor age 32 years (RRID:SAMN 22441940). Islets from ADI were used for DDR induction, GSIS and western blots were from a healthy nondiabetic Caucasian male donor age 55 (RRID:

bioRxiv preprint doi: https://doi.org/10.1101/2021.06.07.447428; this version posted December 22, 2021. The copyright holder for this preprint (which was not certified by peer review) is the author/funder, who has granted bioRxiv a license to display the preprint in perpetuity. It is made available under aCC-BY-NC-ND 4.0 International license.

SAMN23408101). Upon receipt islets were rested in culture for 24 h in RPMI-1640 media containing 10% FBS, 2 mM L-glutamine, 5.5 mM glucose and 1X antibiotic-antimycotic, as previously [7,14]. To induce DDR and senescence, islets were cultured in media containing 50 µM bleomycin (Medchem express) or vehicle (0.2% DMSO) controls for 48 h, followed by removal and culture in drug-free media for 2-5 days, as previously [7]. Islets were then harvested for RNA extraction or protein. For conditioned media, islets were put into serum-free islet media on day 4 post-drug washout, for 24 h and the conditioned media collected. To induce ER stress and UPR, islets were cultured in 1 µM Thapsigargin for 5 h, before harvest for protein extraction.

The human fetal EndoC β cell lines have been previously described [23]. The latest derivative, EndoC-βH5, were purchased from Human Cell Design. These cells are derived from the earlier EndoC-βH3 line [24] and have clonally selected for maximal insulin secretory responses and β cell identity marker expression (Human Cell Design). The βH5 line has undergone tamoxifen-mediated excision of the immortalizing SV40 Large T-antigen and hTERT transgenes as in the earlier EndoC-βH3 cell line to render the cells mature and non-proliferative. βH5 cells were seeded at 3.75 or $4x10^5$ cells per well in 12-well TPP plates treated with gel matrix provided by the supplier (βCOAT) and cultured in serum free media (OPTIβ1) as previously, containing: DMEM that contained 5.6 mM glucose, 2% BSA fraction V, 50 µM 2-mercaptoethanol, 10 mM nicotinamide, 5.5 µg/ml transferrin, 6.7 ng/ml selenite, 100 U/ml penicillin, and 100 µg/ml streptomycin (supplied by Human Cell Design). After thawing cells, media was changed within 4 h after cells attached and was replaced with media containing 0.1% DMSO (vehicle control) or 35 µM bleomycin for 48 h. Following drug treatment, the media was replaced

bioRxiv preprint doi: https://doi.org/10.1101/2021.06.07.447428; this version posted December 22, 2021. The copyright holder for this preprint (which was not certified by peer review) is the author/funder, who has granted bioRxiv a license to display the preprint in perpetuity. It is made available under aCC-BY-NC-ND 4.0 International license.

with fresh media for an additional 2 days of culture or cells were harvested immediately after drug treatment for western blot. In a second experiment cells were cultured in normal growth media for an additional 4 days after drug removal and media was replaced on day 4 to generate conditioned media for 24 h for Luminex assays

2.3 Western blot analysis.

Whole cell extracts were prepared with RIPA buffer (ThermoFisher) in the presence of 1X protease and phosphatase inhibitor cocktail (ThermoFisher) and protein was quantified with the BCA assay (ThermoFisher). Testis tissue from C57BL6/J 3 month old mice was a gift from Dr. C. Doucette (University of Manitoba). Approximately 3-10 µg of total protein from testis, MIN6 or NIT1 cells, human islets, or EndoC-βH5 cells treated as indicated (equal amounts per sample for each experiment) were electrophoresed on precast 4-12% Bis-Tris Plus Bolt Mini gradient gels and electroblotted onto nitrocellulose membranes with the Mini Bolt-iBlot2 system (ThermoFisher). Membranes were blocked in 5% non-fat milk in Tris buffered saline with 0.1% Tween-20 (TBST) for 1 h at room temperature. Primary antibodies used for westerns and dilutions used are indicated in **Supplementary Table 3**. Primary antibodies were incubated on membranes in TBST overnight at 4°C, washed three times for 5 minutes in TBST and detected with HRP-conjugated secondaries (Jackson Immunoresearch, diluted 1:50,000-1:100,000) after incubation for 1 h at room temperature in 5% non-fat milk in TBST. Membranes were washed three times for 5 minutes in TBST and were then incubated with SuperSignal West Pico Plus ECL (Thermo Fisher). Membranes were developed after exposure to X-ray film (Fuji Medical)

bioRxiv preprint doi: https://doi.org/10.1101/2021.06.07.447428; this version posted December 22, 2021. The copyright holder for this preprint (which was not certified by peer review) is the author/funder, who has granted bioRxiv a license to display the preprint in perpetuity. It is made available under aCC-BY-NC-ND 4.0 International license.

and two or three exposures were collected to ensure signals were not saturated. Densitometry was performed using ImageJ to quantify band intensities relative to β-Actin as a loading control on each blot.

2.4 SA-βgal activity assay.

SA-βgal activity in MIN6 and NIT1 cells was detected using a commercial kit (Cell Signaling Technology) according to the product instructions. Cells were subsequently washed in PBS and imaged on an EVOS color brightfield imager.

2.5 EdU labeling assay.

EdU incorporation was measured as an assay for DNA synthesis using a commercial kit (Abcam) according to the product instructions modified for adherent cells. Briefly, MIN6 or NIT1 cells were induced to senescence as indicated above and on the day of drug removal (72 h post-treatment) cells were incubated with media containing 5 µM EdU for 3 h at 37°C and 5% CO_2. Cells were subsequently washed with d-PBS, trypsinized, counted and resuspended at 1-5 x 10^6 cells/ml in d-PBS. The zombie NIR fixable viability kit (BioLegend) was used according to the manufacturer's instructions prior to fixation in 4% formaldehyde. After fixation, cell pellets were washed twice using cell staining buffer (BioLegend), permeabilized and treated with EdU detection solution. After two more washes, cells were filtered through a 70 µm strainer (ThermoFisher Scientific) into 5 mL flow tubes (ThermoFisher Scientific). Flow cytometry was

bioRxiv preprint doi: https://doi.org/10.1101/2021.06.07.447428; this version posted December 22, 2021. The copyright holder for this preprint (which was not certified by peer review) is the author/funder, who has granted bioRxiv a license to display the preprint in perpetuity. It is made available under aCC-BY-NC-ND 4.0 International license.

performed on an Attune acoustic focusing cytometer with a gating strategy as follows: FSC-A/SSC-A (cells), FSC-A/FSC-W (single cells), Zombie Near IR-negative (RL3, live cells) and EdU-positive (RL1). Approximately 4-10,000 live cells were scored per sample.

2.6 Luminex assays.

Conditioned media (CM) was collected by culturing cells or islets in growth media lacking FBS for 18-24 h. CM was collected, clarified by centrifugation (3000g for 5 minutes at room temperature) and either used immediately or stored at 4°C for up to 2-3 weeks. Luminex assays were carried out on CM from cells treated as indicated using a custom magnetic bead kit that included mouse SASP factors IL-6, Serpine1 and Igfbp3, or human SASP factors CXCL1, IL-8, IGFBP4, GDF-15, or TNFRSF10C (R&D systems). 50 µl of CM was assayed on a Bio-Plex 200 luminex platform (Bio-Rad) as previously [7,14] and secreted amounts in 1-2 ml of CM were normalized to viable cell counts to calculate amount secreted per 100,000 cells or for human islets secretion was normalized to total RNA content. Alternatively, media was spin-concentrated using a 3 kDa MWCO centrifugal unit (Millipore-Sigma) and the concentrated conditioned media was analyzed by Luminex.

2.7 RNA extraction and quantitative RT-PCR.

bioRxiv preprint doi: https://doi.org/10.1101/2021.06.07.447428; this version posted December 22, 2021. The copyright holder for this preprint (which was not certified by peer review) is the author/funder, who has granted bioRxiv a license to display the preprint in perpetuity. It is made available under aCC-BY-NC-ND 4.0 International license.

Total RNA was extracted from MIN6, NIT1, human islets or EndoC-βH5 cells using a commercial column-based purification with DNAse I treatment (Direct-Zol RNA MicroPrep with Trizol Reagent, Zymo Research). RNA was quantified by Nanodrop spectrophotometer (ThermoFisher Scientific). Approximately 50-300 ng of total RNA was used for cDNA synthesis with random primers (LunaScript SuperMix Kit, New England Biolabs), depending on the cells used. qPCR was carried out on a Bio-Rad CFX96 using Luna Universal qPCR Master Mix (New England BioLabs). Primers used for qPCR were previously validated from other studies and are indicated in **Supplementary Table 3**.

2.8 RNA-seq on human islets.

Approximately 1 µg of total RNA from bleomycin and vehicle-treated islets (n = 3 biological replicates per group) at 4 days post-drug removal was submitted for paired-end RNA sequencing on Illumina Nova-Seq 6000 platform by a commercial service provider, LC Sciences. Total RNA was quality checked and ribosomal RNA depleted. Libraries were prepared with Illumina TruSeq-stranded total RNA sample protocol and quality checked by Agilent BioAnalyzer 2100 High Sensitivity DNA Chip. Cutadapt [25] and perl scripts were used to filter adapter contamination and undetermined bases. Sequences were quality checked with FastQC (https://www.bioinformatics.babraham.ac.uk/projects/fastqc)and mapped to the human genome (version 96) using Bowtie2 [26] and HISAT2 [27]. Mapped reads were assembled for each sample with StringTie [28] . A comprehensive transcriptome was prepared using perl scripts and gffcompare (https://github.com/gpertea/gffcompare/). StringTie and edgeR[29] were used to estimate transcript expression levels. LncRNAs

bioRxiv preprint doi: https://doi.org/10.1101/2021.06.07.447428; this version posted December 22, 2021. The copyright holder for this preprint (which was not certified by peer review) is the author/funder, who has granted bioRxiv a license to display the preprint in perpetuity. It is made available under aCC-BY-NC-ND 4.0 International license.

were identified based on filtering transcripts overlapping with known mRNAs, known lncRNAs and transcripts <200 bps. CPC [30] and CNCI [31] were used to predict transcripts coding potential. Transcripts with CPC score <-1 and CNCI score <0 were removed. Remaining transcripts were considered lncRNAs. StringTie was used to perform differential expression level analysis for mRNAs and lncRNAs by calculating FPKM (total exon fragments/mapped reads(millions) x exon length (kb)). A complete list of differentially and all expressed genes is shown in Supplementary Table 1. A complete list of differentially expressed lncRNAs and novel lncRNAs is found in Supplementary Table 2. Differentially expressed mRNAs and lncRNAs were selected with log2 fold-change >1 or <-1 between vehicle control and bleomycin treatment and parametric F-test comparing linear nested models ($p < 0.05$) by edgeR. GO and KEGG analysis was performed using by hypergeometric distribution fitting ($p < 0.05$) from gene ontology terms (http://www.geneontology.org) and KEGG pathways (http://www.kegg.jp).

2.9 Static glucose stimulated insulin secretion assays.

Glucose-stimulated insulin secretion was measured from MIN6 and NIT1 cells and human islets according to standard methods with minor changes [32,33]. For mouse β cell lines, cells were seeded as indicated above cultured with vehicle or etoposide for 72 h to induce senescence. At the 72 h post-treatment timepoint, cells were washed in and incubated for 1 h in a tissue culture incubator in Krebs-Ringer Bicarbonate (KRB) buffer (128.8 mM NaCl, 4.8 mM KCl, 1.2 mM KH_2PO_4, 1.2 mM $MgSO_4$, 2.5 mM $CaCl_2$, 5 mM $NaHCO_3$, 10 mM HEPES) containing 0.1% BSA fraction V (Millipore-Sigma). Then cells were incubated for 1 h in fresh KRB buffer with BSA as above containing 0 mM glucose

bioRxiv preprint doi: https://doi.org/10.1101/2021.06.07.447428; this version posted December 22, 2021. The copyright holder for this preprint (which was not certified by peer review) is the author/funder, who has granted bioRxiv a license to display the preprint in perpetuity. It is made available under aCC-BY-NC-ND 4.0 International license.

as the low glucose condition, followed by 1 h in KRB with BSA containing 20 mM glucose as the high glucose condition. Total insulin content was collected by lysing cells in an acidified ethanol solution (0.15 M HCl, 95% ethanol). Human islets were treated in n = 6 biological replicates of vehicle control (DMSO) or 50 μM bleomycin for 48 h to induce senescence, followed by culture in drug-free media for an additional 4 days. At day 5 post-drug removal, islets were washed in KRB + 0.1% BSA containing 2 mM glucose (low glucose) and incubated in the low glucose buffer for 1 h. Islets were then washed into KRB + 0.1% BSA containing 20 mM glucose for 1 h (high glucose buffer) and supernatants of the 2 mM and 20 mM glucose buffers were collected. For both mouse β cell lines and human islets, aliquots of the low and high glucose supernatants and the insulin content extracts were collected and spun at 3000g for 5 minutes at 4°C and stored at -20°C or used immediately for mouse or human insulin ELISAs (Mercodia) with appropriate dilutions (1:10-1:50 for supernatants, 1:100-1000 for insulin content). Insulin secretion in the supernatants were quantified as a function of total insulin content from each sample.

2.10 Statistical analysis.

All statistical analyses were performed using GraphPad Prism version 9.3.1 with a minimum of n = 3 biological replicates per sample group. Statistical comparisons were performed with two-tailed unpaired T-tests, or two-way ANOVAs where indicated, and were considered significant at $p < 0.05$.

3. Results

3.1 Sub-lethal DNA damage with etoposide leads to senescent phenotypes in NIT1 cells

bioRxiv preprint doi: https://doi.org/10.1101/2021.06.07.447428; this version posted December 22, 2021. The copyright holder for this preprint (which was not certified by peer review) is the author/funder, who has granted bioRxiv a license to display the preprint in perpetuity. It is made available under aCC-BY-NC-ND 4.0 International license.

To investigate whether DNA damage leads to senescence phenotypes in β cells relevant to T1D, we used the NIT1 β cell line, derived from an insulinoma in the T1D-susceptible NOD/LtJ mouse strain [21]. For comparison, we also examined the MIN6 β cell line derived from the non-T1D susceptible C57BL6 strain [20], which was recently shown to develop some senescent phenotypes in response to DNA damage with bleomycin [34], although a comprehensive investigation in this line was not performed. We induced DNA double-strand breaks using the topoisomerase II (TopoII) poison etoposide [35], as this drug has been used in the clinic to treat insulinomas [36] and leads to an increased burden of unrepaired endogenous DNA double-strand breaks due to inhibited ligation after cleavage by endogenous TopoII enzymes. Of the two type II topoisomerase family members, we found that TopoIIα was expressed in both MIN6 cells and NIT1 cells, while TopoIIβ was expressed only in MIN6 (**Supplementary Figure 1A**) confirming that these cells express the target of this drug.

MIN6 or NIT1 cells were cultured in etoposide for 3 days, followed by drug removal to assay early senescent phenotypes or culturing the cells in drug-free media for an additional 5-14 days to assay late senescent phenotypes (**Figure 1A**). We titrated the doses of etoposide to maintain viability throughout the treatment and culture period. While MIN6 cells tolerated 2 µM with >60% viability for up to 14 days post-drug removal, NIT1 could only survive in up to 0.5 µM for 7-9 days post-drug removal (**Figure 1B**) and similar results were obtained using 0.25 µM etoposide. Viability for both cell lines was maintained at ~80-90% during 72 h of drug treatment (**Figure 1B**) but cell counts were significantly lower in the etoposide-treated cells as compared with controls

bioRxiv preprint doi: https://doi.org/10.1101/2021.06.07.447428; this version posted December 22, 2021. The copyright holder for this preprint (which was not certified by peer review) is the author/funder, who has granted bioRxiv a license to display the preprint in perpetuity. It is made available under aCC-BY-NC-ND 4.0 International license.

(**Supplementary Figure 1B**), suggesting that while some cell death was occurring, there was also a proliferation arrest during drug treatment period.

β cells with DNA damage in vivo activate a canonical DDR involving the ATM-p53-21 pathway and phosphorylated KAP1^{Ser824} and phosphorylated Histone H2A.X^{Ser139} (gamma-H2A.X) [7,19,37,38]. Therefore, we next characterized DDR activation in MIN6 and NIT1 cells 24 h after etoposide treatment (**Figure 1C**). MIN6 cells exhibited a coordinated DDR with significant increases in phosphorylated ATM^{Ser1981}, total p53, gamma-H2A.X, phosphorylated KAP1^{Ser824} and p21 (**Figure 1C**). In contrast, while NIT1 cells had increased activated ATM, phosphorylated KAP1 and induction of p21, there was no increase in total p53 or gamma-H2A.X (**Figure 1C**). Activated p53 (phospho-p53^{Ser15}) was also detected in both undamaged and etoposide-treated MIN6 and NIT1 cells, but was not significantly increased relative to total p53 levels (**Supplementary Figure 2**). Total p53 and gamma-H2A.X were already abundant in undamaged NIT1 and MIN6 cells (**Figure 1C)**. Etoposide treatment also reduced the percent of MIN6 and NIT1 cells replicating DNA as indicated by a lower proportion of cells labeled with EdU at 72 h post-drug treatment (**Figure 1D**) consistent with a growth arrest. Similarly, etoposide treated MIN6 cells developed an enlarged flattened morphology with strong SA-βgal activity by 5 days after drug removal, however, while NIT1 cells showed enlarged flattened morphology, they did not stain positive for SA-βgal activity at the same time point (**Figure 1E**). Taken together, these data show that NIT1 cells are more sensitive to DNA damage than MIN6 and that sub-lethal DNA double-strand break damage triggers canonical DDR activation, growth arrest and senescence-related morphology changes.

bioRxiv preprint doi: https://doi.org/10.1101/2021.06.07.447428; this version posted December 22, 2021. The copyright holder for this preprint (which was not certified by peer review) is the author/funder, who has granted bioRxiv a license to display the preprint in perpetuity. It is made available under aCC-BY-NC-ND 4.0 International license.

3.2 Cdkn1a but not Cdkn2a is upregulated in growth arrested NIT1 cells

We next assessed whether CDK inhibitors p21 and/or p16^{Ink4a} were upregulated at later stages after drug removal in NIT1 cells (**Figure 2**). Notably, at the 72 h post-treatment timepoint, *Cdkn1a* but not *Cdkn2a* was upregulated in MIN6 cells and this persisted into late stage senescence at 14 days post-drug removal (**Figure 2A**). Similarly, NIT1 cells also upregulated *Cdkn1a* expression at 72 h post-treatment and 7 days post-drug removal and also showed no upregulation of *Cdkn2a* (**Figure 2B**). Elevated p21 expression was also reflected at the protein level 72 h post-treatment and 7 or 14 days post-drug removal in both lines, whereas again p16^{Ink4a} was not detected (**Figure 2C and 2D**). We also assessed the expression of Bcl-2, which is selectively upregulated during β cell senescence in T1D and confers a prosurvival phenotype [7]. Notably, Bcl-2 was below the detection limit in control or etoposide treated MIN6 cells or NIT1 cells, despite robust expression in mouse testis as a positive control (**Supplementary Figure 3**). Taken together these data suggest that senescent growth arrest in NIT1 involves p21 but not p16^{Ink4a} and does not involve Bcl-2 upregulation.

3.3 Differences in SASP development and UPR in MIN6 and NIT1 cells following DNA damage

SASPs are cell-type and stressor-dependent, dynamic programs of secreted cytokines, chemokines, matrix proteases, shed receptors, growth factors, microRNAs and extracellular vesicles that are immunogenic and exert the paracrine effects of senescent cells within the tissue microenvironment [39–41]. In senescent β cells during pathogenesis of T1D in NOD mice, SASP comprises a wide variety factors such as

bioRxiv preprint doi: https://doi.org/10.1101/2021.06.07.447428; this version posted December 22, 2021. The copyright holder for this preprint (which was not certified by peer review) is the author/funder, who has granted bioRxiv a license to display the preprint in perpetuity. It is made available under aCC-BY-NC-ND 4.0 International license.

interleukins (IL-6), chemokines (Cxcl10), growth factors (Igfbp3), and matrix metalloproteases and protease inhibitors (Mmp2, Serpine1) [7,14]. To determine whether etoposide-induced DDR in NIT1 cells led to a SASP resembling primary β cells in T1D, we assayed a panel of SASP factors we previously identified NOD mouse β cells by a combination of western blot and luminex secretion assays (**Figure 3**). Western blot of proenzyme and cleaved active Mmp2 isoforms revealed that etoposide treatment led to increased pro-Mmp2 levels in both MIN6 and NIT1 cells (**Figure 3A and 3B**). Luminex assays for SASP factors IL-6, Serpine1 and Igfbp3 [7] on conditioned media showed dramatically increased secretion of Serpine1 and Igfbp3, but not IL-6 from senescent NIT1 cells as compared with controls whereas none of these factors were secreted by late-stage senescent MIN6 cells (**Figure 3C and 3D**). Next, we determined whether induction of DDR and senescence would impact the UPR, a different β stress response implicated in T1D [4]. We validated antibodies for UPR mediators phospho-IRE1α^{Ser724} (activated IRE1α) and total IRE1α, total PERK and total ATF6α (90 kDa uncleaved form) by western blot on primary human islets treated with 1 μM Thapsigargin for 5 h, which led to increased levels of these UPR factors (**Supplementary Fig. 4**). Western blot analysis revealed induced p21 at 72 h post-etoposide treatment in both lines as expected, however, MIN6 cells also showed reduced phosphorylated and total IRE1α levels, whereas NIT1 cells showed no significant differences in any of these UPR mediators (**Figure 3E and 3F**), suggesting that DDR and early senescence leads to different effects on UPR mediators in MIN6 versus NIT1 cells. Taken together these data reveal that senescence induction leads to differences in SASP and UPR mediators between MIN6 and NIT1 cells.

bioRxiv preprint doi: https://doi.org/10.1101/2021.06.07.447428; this version posted December 22, 2021. The copyright holder for this preprint (which was not certified by peer review) is the author/funder, who has granted bioRxiv a license to display the preprint in perpetuity. It is made available under aCC-BY-NC-ND 4.0 International license.

3.4 RNA-seq reveals DDR and senescence transcriptional program of human islets

To provide an unbiased analysis of the transcriptional program following DDR and senescence in human islets, we next performed RNA-seq on senescent and control human islets cultured ex vivo using our previous human islet senescence model [7,14] (**Figure 4**). Primary islets isolated from a healthy female donor were cultured with bleomycin to induce DNA damage for 48 h and total islet RNA from the samples was extracted at 4 days post-drug removal for paired-end RNA-seq (**Figure 4A**). This timepoint is typically 1 day prior to the detection of SASP secretion in this model [7,14], and we reasoned that transcriptional changes in SASP genes would precede increased protein secretion, as SASP is controlled transcriptionally [14,15]. Differential expression analysis revealed 1690 genes significantly downregulated ≥0.5-fold and 201 genes significantly upregulated ≥2-fold ($p < 0.05$) (**Figure 4B**). A complete list of all genes with detected expression levels as fragments per kilobase per million reads (FPKM) are listed in Supplementary Table 1. Differentially expressed genes were enriched for gene ontology (GO) terms including 'cell division' and 'cell cycle' and KEGG pathways 'cell cycle', 'p53 signaling pathway' and 'PI3K-Akt signaling pathway' (**Figure 4C**, **Supplementary Figure 5A**). Genes involved in proliferation and cell cycle progression such as *MIK67, RRM2, TOP2A, CCNA2*, *CCNB2, MCM10, CDK1* were significantly downregulated (**Figure 4D**) and p53 DDR pathway genes including *SPATA18, DDB2, GADD45A, GADD45G, ACER2, ZMAT3* [42] were significantly upregulated (**Figure 4E**). In addition, p53 target gene *CDKN1A* was upregulated, but not other cyclin-dependent kinase inhibitor genes such as *CDKN2A*, *CDKN1B*, *CDKN1C, CDKN1D* or *CDKN2B* (**Figure 4E and Supplementary Table 1**). Gene expression changes associated with early senescence also occurred, including downregulation of *LMNB1* and *HMGB2*

bioRxiv preprint doi: https://doi.org/10.1101/2021.06.07.447428; this version posted December 22, 2021. The copyright holder for this preprint (which was not certified by peer review) is the author/funder, who has granted bioRxiv a license to display the preprint in perpetuity. It is made available under aCC-BY-NC-ND 4.0 International license.

(**Figure 4E**) both of which occur during p53-mediated senescence induction in other cell types [43,44]. In addition to mRNAs, we also noted several small noncoding RNAs that were differentially expressed. These included *MIR34A*, a microRNA involved in senescence [45], along with *MIR3687-2* , *MIR3648-2, SNORA46 SNORA84, SNORD94* and *SNORD14B* which were all upregulated and *MIR22, MIR222, MIR143, MIR1-2*, *DNMOS3* were downregulated (**Supplementary Table 1**). We also found a group of previously annotated long noncoding RNAs (lncRNAs) that were differentially expressed and a group of predicted novel lncRNAs in bleomycin-treated islets (**Supplementary Table 2**). Notably among the lncRNAs, *DINOL* was found to be upregulated (**Supplementary Table 1**), consistent with its established role in amplifying p53-p21-mediated DDR signaling [46]. Together, these data validate that bleomycin treatment activates a p53-p21 DDR and early senescence transcriptional program in adult human islets.

3.5 DDR and senescence does not alter human islet cell identity genes or UPR genes

To assess the effects of DDR activation and senescence on human β cell/endocrine islet cell function and identity we surveyed genes involved in hormone production and endocrine cell identity (**Figure 4F**). Genes encoding endocrine islet cell hormones and processing enzymes (*INS, GCG, SST, INSR, PCSK1, PCSK2, CPE*) and key beta/islet cell transcription factors (*PDX1, NKX6.1, MAFA, MAFB, NKX2.2, RFX6, ARX*) were not changed (**Figure 4F**). The only exception was upregulation of *PCSK1N*, which encodes proSAAS, an endogenous inhibitor of the PCSK1 hormone processing enzyme that mediates proinsulin cleavage [47] (**Figure 4F**). Furthermore, genes involved in ER

bioRxiv preprint doi: https://doi.org/10.1101/2021.06.07.447428; this version posted December 22, 2021. The copyright holder for this preprint (which was not certified by peer review) is the author/funder, who has granted bioRxiv a license to display the preprint in perpetuity. It is made available under aCC-BY-NC-ND 4.0 International license.

stress and UPR (*XBP1, DDIT3, EDEM1, ERN1, ATF4, ATF6, HSPA5, HSP90B1*) [4], were not significantly changed between control and bleomycin treatment (**Supplementary Figure 5B**). Comparison of the list of differentially expressed genes in our dataset with recently generated human islet RNA-seq datasets during aging [48] and adult human islets treated with the cytokine IFNα [49] showed that there were only 74/385 (~19%) age-related genes in common and only 256/1894 (~13%) IFNα-regulated genes in common, respectively, (**Supplementary Figure 5C, Supplementary Table 1**). This suggested that the transcriptional response during islet DDR activation and senescence is generally different from natural aging and cytokine exposure.

3.5 BCL-2 family genes and SASP genes in islet DDR and senescence

To assess whether islet cells were developing late senescence phenotypes, we next looked at BCL-2 family prosurvival genes and SASP genes. Among the prosurvival family members, *BCL2L1, MCL1* and *BCL2L2* were the only members expressed at appreciable levels in islets, and of these only *BCL2L1* (encoding BCL-XL) was significantly upregulated (**Figure 4G**). Assessment of genes encoding canonical proinflammatory SASP factors such as *IL6, CXCL8, SERPINE1, IGFBP3, CXCL1, IGFBP4, MMP1, MMP2* revealed that the majority of them were either dramatically downregulated or unchanged in bleomycin treated islets relative to controls (**Supplementary Table 1**). However, among the significantly upregulated genes, we noted several previously identified SASP genes encoding secreted factors and cell surface receptors, including *GDF15, CXCL5, CCL11, TNFRSF10C, TNFRSF10A* and *SERPINA6* [16,34,39,50,51] (**Figure 4H**).

3.6 Bleomycin induces DDR and senescence phenotypes in a human β cell line model

bioRxiv preprint doi: https://doi.org/10.1101/2021.06.07.447428; this version posted December 22, 2021. The copyright holder for this preprint (which was not certified by peer review) is the author/funder, who has granted bioRxiv a license to display the preprint in perpetuity. It is made available under aCC-BY-NC-ND 4.0 International license.

To corroborate the p53-p21 pathway transcriptional changes identified by RNA-seq on islets and determine whether increased SASP gene expression is reflected in protein secretion, we carried out western blot for DDR and senescence proteins and Luminex assays on two independent islet preparations at day 5 post-drug removal isolated from adult male donors (**Figure 5A**). Notably, westerns confirmed significantly increased expression of DDR markers phospho-ATM^{Ser1981} and p21 (**Figure 5B**). In addition, Luminex assays revealed increased secretion of previously characterized islet SASP factors IL-8, CXCL1 and IGFPB4 along with newly identified factors TNFRSF10C and GDF-15 (**Figure 5C**). Since islets are a mixed cell population, the direct contribution of β cells to the observed senescent phenotypes cannot be determined. Therefore, we turned to the EndoC-βH5 human β cell line model to determine whether similar phenotypes could be induced in directly in human β cells experiencing DNA damage (**Figure 5D**). EndoC-βH5 cells are the latest derivative of the widely used EndoC human fetal β cell lines [23] that has been clonally selected for maximal Insulin secretion and β cell identity markers and is essentially non-proliferating. After seeding and 2 days in culture, we treated EndoC-βH5 cells for 48 h with vehicle (0.1% DMSO) or 35 µM bleomycin, followed by drug removal and additional culture for 2-5 days to monitor early and late senescence phenotypes (**Figure 5D**). Notably, 48 h after bleo treatment, these cells activated DDR signaling as judged by western blot analysis for phospho-ATM^{Ser1981}, gamma-H2A.X and p21 (**Figure 5E**). QRT-PCR demonstrated a sustained expression of *CDKN1A* 2 days after drug removal, but again *CDKN2A* was unaffected (**Figure 5F**). We also confirmed upregulation of SASP and BCL-2 family genes (*CXCL8* and *BCL2L1*) (**Figure 5F**) suggesting development of late senescence phenotypes

bioRxiv preprint doi: https://doi.org/10.1101/2021.06.07.447428; this version posted December 22, 2021. The copyright holder for this preprint (which was not certified by peer review) is the author/funder, who has granted bioRxiv a license to display the preprint in perpetuity. It is made available under aCC-BY-NC-ND 4.0 International license.

starting at 2 days post-drug removal. To determine whether SASP factor secretion was occurring we monitored secretion of islet SASP factors IL-8, IGFPB4, CXCL1 and newly identified factors TNFRSF10C and GDF-15 by Luminex on conditioned media at day 5 post-drug removal. Of these factors, TNFRSF10C was not detectable and only GDF-15 showed significantly increased secretion (**Figure 5G**). Taken together, these data suggest that DNA damage is sufficient to induce senescent phenotypes directly in human β cells.

3.7 Senescence decreases β cell insulin content

Finally, we explored the effect of DDR and senescence on insulin secretion (**Figure 6**). Surprisingly, induction of DDR and senescence in MIN6 and NIT1 cells led to abnormally increased GSIS with elevated basal and glucose-stimulated insulin secretion (GSIS) from both lines (**Figure 6A**). Early senescent NIT1 and MIN6 cells also showed significantly reduced insulin content (**Figure 6A**). In contrast, established senescence at day 5 post-drug removal in human islets did not affect GSIS, but led to decreased insulin content (**Figure 6B**). Taken together, these results suggest that DDR and senescence diminishes insulin content and shows different on GSIS in mouse β cell lines as compared with human islets.

4. Discussion

bioRxiv preprint doi: https://doi.org/10.1101/2021.06.07.447428; this version posted December 22, 2021. The copyright holder for this preprint (which was not certified by peer review) is the author/funder, who has granted bioRxiv a license to display the preprint in perpetuity. It is made available under aCC-BY-NC-ND 4.0 International license.

A subpopulation of β cells acquire senescence as a stress response during development and onset of T1D [7], but the triggers/stressors that lead to senescence in this setting are not known. The use of cell culture models has been indispensable for the field of senescence and has been foundational for understanding the mechanisms underpinning this complex process. Since senescent β cells in T1D show DDR activation [7,19] and persistent unrepaired DNA damage is a known inducer of senescence, we carried out studies to determine the extent to which chemically induced DNA damage in the NIT1 cell line derived from the T1D-susceptible NOD mouse strain, adult human islets and EndoC cells recapitulates features of β cell senescence in T1D. We demonstrated that NIT1 cells responded to accumulated endogenous DNA double-strand break damage from low concentrations of etoposide by activating the DDR, growth arrest, developing an enlarged flattened morphology and a SASP resembling what is observed in T1D. There were some notable differences in these phenotypes as compared with MIN6 cells, which did not secrete most of these SASP factors, pointing to the role of genetic background in modifying senescent phenotypes. Consistent with previous findings revealing polymorphisms that reduce the efficiency of DNA double-strand break repair in NOD/ShiLtJ as compared with C57BL10 embryonic fibroblasts [18], NIT1 cells were more sensitive to DNA double-strand break damage as compared with MIN6. In addition, although they were clearly growth arrested and developed an enlarged and flattened morphology, NIT1 cells also did not develop high SA-βgal activity like MIN6 cells and β cell senescence during T1D [7]. Both cell lines had sustained upregulation of *Cdkn1a* expression at the gene and protein levels but not *Cdkn2a*, suggesting that the growth arrest relies on p21 rather than $p16^{Ink4a}$. Furthermore, Bcl-2

bioRxiv preprint doi: https://doi.org/10.1101/2021.06.07.447428; this version posted December 22, 2021. The copyright holder for this preprint (which was not certified by peer review) is the author/funder, who has granted bioRxiv a license to display the preprint in perpetuity. It is made available under aCC-BY-NC-ND 4.0 International license.

was not detected in NIT1 or MIN6 cells and consistent with a lack of prosurvival phenotype, these lines showed declining viability in culture at late stages. Taken as a whole, these results suggest that specific aspects of mouse β cell senescence in T1D, including DDR activation, growth arrest and SASP, but not SA-βgal activity or Bcl-2 prosurvival phenotype can be modeled using NIT1 cells treated with sub-lethal concentrations of etoposide.

Human islets show substantial differences in architecture, metabolism, and proliferative capacity as compared with rodents [52], necessitating the study of β cell DDR and senescence in human models. We previously established a primary human pancreatic islet model for DDR and senescence using the DNA double-strand break agent bleomycin and found that it induces some of the same phenotypes observed during β cell senescence in human T1D donors [7]. However, a systematic interrogation of this model was lacking and it was previously not determined whether β cells contributed to the observed phenotypes. Using an unbiased analysis by RNA-seq, we found that DDR activation and senescence induction by bleomycin treatment of islets resulted in a coordinated p53-p21 transcriptional program, involving downregulation of genes involved in proliferation and cell cycle progression and upregulation of p53-targeted genes. Although there were a small subset of genes in common with other human islet RNA-seq datasets representing natural aging [48] or cytokine exposure [53] the changes during islet DDR activation and senescence were largely distinct. Importantly, the changes in this model occur 4 days after drug removal (6 days post-treatment) and thus reflect a stable phenotypic change rather than an acute response. Notable among

bioRxiv preprint doi: https://doi.org/10.1101/2021.06.07.447428; this version posted December 22, 2021. The copyright holder for this preprint (which was not certified by peer review) is the author/funder, who has granted bioRxiv a license to display the preprint in perpetuity. It is made available under aCC-BY-NC-ND 4.0 International license.

these changes was the robust upregulation of *CDKN1A* (p21) and no increases in *CDKN2A* (p16) expression, consistent with our earlier analysis by qRT-PCR and protein-level changes in senescent β cells of T1D donors [7]. We further corroborated these changes in a human β cell line model, EndoC-βH5 cells, confirming that it can occur directly in β cells. While *CDKN2A* gene expression was not induced in islets after DDR and senescence, $p16^{INK4A}$ protein level is already very abundant in middle-aged adult donor pancreas and islets [7,54,55], thus the gene expression level is likely not an accurate reflection of the protein levels. Remarkably, there were no significant changes in islet cell hormone genes, lineage identity genes, or UPR genes at this timepoint after DDR activation and early senescence. In addition to a p53-p21 transcriptional response in bleomycin-treated islets, we also found evidence for two other senescence phenotypes, BCL-2 family gene upregulation and SASP. We identified selective upregulation of BCL2 family member gene *BCL2L1* in bleomycin treated islets. The BCL-2 family of anti-apoptotic proteins confer a prosurvival phenotype on senescent cells and *BCL2L1* encodes BCL-XL, which is known to be upregulated at the mRNA and protein level in other cell types during senescence [56,57]. Thus, it will be interesting to investigate whether BCL-XL is upregulated during β cell senescence in T1D donors and confers a prosurvival phenotype to senescent human β cells.

While many of the classical proinflammatory SASP genes were downregulated during DDR-mediated senescence in islets, a subset of previously identified TGFβ-related SASP genes encoding secreted factors and shed receptors [58] were significantly upregulated at the RNA level. Notable among them were *GDF15* and *TNFRSF10C*, which were also validated at the protein level in secretion assays to monitor SASP.

bioRxiv preprint doi: https://doi.org/10.1101/2021.06.07.447428; this version posted December 22, 2021. The copyright holder for this preprint (which was not certified by peer review) is the author/funder, who has granted bioRxiv a license to display the preprint in perpetuity. It is made available under aCC-BY-NC-ND 4.0 International license.

GDF15 was recently identified as a β cell SASP factor in mice in a T2D model [34] and an anti-apoptotic factor in human islets, conferring protection from cytokine-induced apoptosis [59]. Importantly, GDF15 has also been linked to age-related senescence and was recently suggested as part of a biomarker panel for senescence-related inflammation [39]. Given its potential role as an anti-apoptotic factor, it will be of interest to determine whether GDF15 confers a prosurvival phenotype on senescent β cells and/or modulates immune-mediated cytoxicity of β cells. Additionally, we found TNFRSF10C, which is a putative decoy receptor to be upregulated both at the RNA and protein levels and secreted following DDR and senescence induction from islets. Given the role of this receptor in inhibiting extrinsic apoptosis in the context of cancer [60], its increased secretion from senescent islet cells may play a role in protecting these cells from immune attack. Thus, we demonstrated that transcriptional upregulation of islet SASP components such as TNFRSF10C and GDF15 is linked with increased SASP secretion. Interestingly, when our islet SASP panel (IL-8, CXCL1, IGFBP4, TNFRSF10C, GDF15) was interrogated in an EndoC human β cell line model for DDR and senescence, we only found GDF15 to be increased in secretion. This may be due to a variety of reasons, such as: 1) differences in β cell maturity between human islet β cells and EndoC cells, 2) effects of different genetic background polymorphisms and/or 3) secretion from non-β cells in the islet. Further investigations will be required to catalogue the similarities and differences between SASP in human islets as compared with EndoC β cell lines and it would be advantageous to sort purify β cells from human islet undergoing DDR and senescence to more closely quantify differences in secretion.

bioRxiv preprint doi: https://doi.org/10.1101/2021.06.07.447428; this version posted December 22, 2021. The copyright holder for this preprint (which was not certified by peer review) is the author/funder, who has granted bioRxiv a license to display the preprint in perpetuity. It is made available under aCC-BY-NC-ND 4.0 International license.

Using our mouse β cell lines and human islet senescence culture models, we determined whether insulin secretion was altered by DDR activation and senescence. Previous work has shown that age-related senescence improves β cell function [54]. However, treatment of euglycemic NOD mice with senolytic compounds to remove senescent β cells does not significantly affect glucose tolerance in vivo or static GSIS on isolated islets ex vivo [7]. In contrast, treatment of T2D mouse models with senolytic compounds improves β cell function [13], although there is likely to be additional effects on senescent cells in other tissues in T2D models [61]. These studies suggest a variety of potential effects of senescence on β cell insulin secretory function, depending on the context and type of senescence. In the present study, GSIS assays revealed an abnormal hypersecretory response during DDR and early senescence in MIN6 and NIT1 cells, where both basal and stimulated insulin secretion was elevated, concomitant with diminished insulin content. Surprisingly, GSIS was not significantly impaired at the day 5 timepoint of DDR-mediated senescence in human islets. However, a decreased insulin content phenotype was apparent, similar to MIN6 and NIT1 cells. *INS* mRNA levels were not significantly different between control and senescent islets as determined by RNA-seq, suggesting that the decreased insulin content may be due to post-transcriptional changes, such as crinophagy or selective insulin granule degradation [62]. Nevertheless, the diminished insulin content phenotype during senescence may be reflective of a progressive functional impairment. Further studies will be required to interrogate the mechanisms involved in these β cell functional changes during DDR and senescence. In conclusion, our findings generally substantiate sub-lethal DNA double-strand break damage in mouse NIT1 cells and

bioRxiv preprint doi: https://doi.org/10.1101/2021.06.07.447428; this version posted December 22, 2021. The copyright holder for this preprint (which was not certified by peer review) is the author/funder, who has granted bioRxiv a license to display the preprint in perpetuity. It is made available under aCC-BY-NC-ND 4.0 International license.

human islets and EndoC-βH5 cells as culture models for some of the key phenotypes of β cell senescence during T1D. Despite their limitations, these models will be useful for further dissecting the molecular mechanisms and functional consequences of senescence and its contributions to the pathogenesis of T1D.

Acknowledgements. The authors thank Dr. Anil Bhushan at University of California San Francisco (UCSF) supported by NIH R01DK121794 and R01DK118099, for providing IIDP human donor islets and resources for PJT to carry out the RNA-seq on human islets while a postdoctoral fellow.

CRediT authorship contribution statement

Gabriel Brawerman: Conceptualization, Methodology, Investigation, Writing - review & editing. **Jasmine Pipella:** Methodology, Investigation, **Peter J. Thompson:** Conceptualization, Formal analysis, Methodology, Investigation, Resources, Writing - original draft, Writing - review & editing, Visualization, Supervision, Funding acquisition.

Declaration of Competing Interest

The authors declare that there are no conflicts of interest.

Availability of Data and Materials.

bioRxiv preprint doi: https://doi.org/10.1101/2021.06.07.447428; this version posted December 22, 2021. The copyright holder for this preprint (which was not certified by peer review) is the author/funder, who has granted bioRxiv a license to display the preprint in perpetuity. It is made available under aCC-BY-NC-ND 4.0 International license.

The RNA-seq raw data and processed data files described in this study are publicly available on NCBI GEO Accession number GSE176324. Expression data tables are also available in Supplementary Information.

Funding

This study was supported by start-up funds awarded to PJT from the University of Manitoba and the Children's Hospital Research Institute of Manitoba and a grant from the University of Manitoba Research Grants Program.

Figure Legends.

Figure 1. Sub-lethal DNA damage with etoposide induces DDR, growth arrest and senescent morphology in MIN6 and NIT1 cells.

(A) MIN6 cells (derived from C57BL6 mouse beta cell tumor) or NIT1 cells (derived from NOD/LtJ mouse beta cell tumor) were seeded and treated with etoposide (2 µM for MIN6, 0.25-0.5 µM for NIT1) or vehicle control (DMSO) for 72 hrs. Drug was removed by changing cells into fresh media, and cells were cultured an additional 5-14 days before final harvests. Early senescence phenotypes were monitored at 24-72 hrs post-etoposide treatment and late phenotypes were assayed at 5-14 days post drug removal.

B) Cell viability was scored at 24 or 72 hrs after etoposide treatment and 7 or 14 days post-drug removal. Data are mean ± SD of n = 3-6 biological replicates.

C) Western blot analysis and relative quantifications of DDR activation markers in MIN6 and NIT1 cells at 24 h post etoposide or vehicle treatment. Data are mean ± SD of n = 3 biological replicates.

D) EdU labeling flow cytometry assay for DNA replication at 72 hrs post-etoposide or vehicle control treatment of MIN6 or NIT1 cells. 'Ctrl' indicates a no EdU negative control population of cells. Data are mean ± SD of n = 3 biological replicates.

E) Representative images of Xgal staining for SA-βgal activity in MIN6 and NIT1 cells at day 5 post-drug removal. Scale bar = 30 µm.

*$p < 0.05$, **$p < 0.005$, ***$p < 0.0005$, ****$p < 0.00005$, unpaired two-tailed T-tests.

bioRxiv preprint doi: https://doi.org/10.1101/2021.06.07.447428; this version posted December 22, 2021. The copyright holder for this preprint (which was not certified by peer review) is the author/funder, who has granted bioRxiv a license to display the preprint in perpetuity. It is made available under aCC-BY-NC-ND 4.0 International license.

Figure 2. Induction of *Cdkn1a* but not *Cdkn2a* at mRNA and protein level in etoposide treated MIN6 and NIT1 cells

A) qRT-PCR analysis of *Cdkn1a* and *Cdkn2a* expression normalized to *Gapdh* in MIN6 cells at 72 hrs post-etoposide or vehicle treatment or 14 days post-drug removal (as from Fig. 1). Data are mean ± SD of n = 3 biological replicates.

B) qRT-PCR analysis as in B) except on NIT1 cells at 72 hrs and 7 days post-drug removal.

C) Western blot of p21 and $p16^{Ink4a}$ on whole cell extracts from MIN6 cells treated with 2 µM etoposide or vehicle control 14 days post-drug removal, Actin was a loading control and whole cell extract from 3 month old C57BL6 mouse testes was a positive control for p21 and p16. P21 quantification relative to actin is mean ± SD of n = 3 biological replicates. Data are mean ± SD of n = 3 biological replicates.

D) Western blot of p21 on whole cell extracts from NIT1 cells treated with 0.25 µM etoposide or vehicle at 6 days post-drug removal. Data are mean ± SD of n = 3 biological replicates.

For all panels, *$p < 0.05$, **$p < 0.005$, ***$p < 0.0005$, ns = not significant, two-tailed T-tests.

Figure 3. Differences in SASP development and UPR in MIN6 and NIT1 cells following etoposide treatment.

A) and B) Western blot analysis of Pro-Mmp2 (70 kDa) and cleaved/activated Mmp2 (62 kDa) on whole cell extracts from MIN6 or NIT1 cells treated with vehicle or etoposide as indicated. Quantification shows relative Pro-Mmp2 or Cleaved Mmp2 to Actin, mean ± SD of n = 3 biological replicates.

C) and D) Luminex assay of secreted SASP factors IL-6, Serpine1 and Igfbp3 in serum-free conditioned media from MIN6 or NIT1 cells treated as indicated at timepoints indicated. Data are mean ± SD from n = 3 biological replicates.

E) and F) Western blot analysis of UPR mediators phosphorylated and total IRE1α, total PERK and total ATF6α in MIN6 and NIT1 cells at 72h post-treatment with etoposide. p21 levels were used as a positive control and β-Actin was a loading control. Data are mean ± SD of n = 3 biological replicates. Asterisk on the blots indicates a non-specific band for the PERK blots.

For all panels, *$p < 0.05$, **$p<0.005$, ***$p<0.0005$, ns = not significant, two-tailed T-tests

bioRxiv preprint doi: https://doi.org/10.1101/2021.06.07.447428; this version posted December 22, 2021. The copyright holder for this preprint (which was not certified by peer review) is the author/funder, who has granted bioRxiv a license to display the preprint in perpetuity. It is made available under aCC-BY-NC-ND 4.0 International license.

Figure 4. RNA-seq analysis reveals activation of the p53-p21 transcriptional program during DDR-mediated senescence in human islets.

A) Overview of human islet DDR and senescence model. Islets isolated from a 44 year-old female donor were rested overnight and then divided into a total of 6 wells and cultured in the presence of vehicle (DMSO) or 50 µM bleomycin for 48 h (n = 3 biological replicates per group). The islets were then transferred to fresh drug-free media and cultured an additional 4 days prior to harvesting on day 5 post-drug removal for RNA extraction and paired-end RNA-seq.

B) Volcano plot of differentially expressed genes ($p < 0.05$) indicating 1690 genes downregulated ≤0.5-fold and 201 genes upregulated ≥2-fold in bleomycin treated islets compared to controls.

C) Significant GO terms of differentially expressed genes.

D) Plot of normalized expression levels (FPKM) of selected significantly downregulated proliferation and cell cycle genes.

E) Plot of normalized expression levels of significantly upregulated p53-p21 DDR genes and two early senescence genes (*LMNB1* and *HMGB2*).

F) Plot of normalized expression levels of selected islet cell identity and hormone genes. None of these genes were differentially expressed except *PCSK1N* which was significantly upregulated in bleo versus control (*$p < 0.05$).

G) Plot of selected BCL-2 family anti-apoptotic genes. Only *BCL2L1* was significantly upregulated, (*$p < 0.05$).

H) Plot of selected significantly downregulated proinflammatory SASP genes and significantly upregulated SASP genes.

Figure 5. Validation of DDR and SASP activation in human islets and the EndoC-βH5 human β cell line.

A) Overview of experiment on human islets. Islets from adult male donors (ages 32 or 55) were treated as indicated and harvested for western blot and Luminex assays.

B) Western blot analysis of DDR and senescence proteins on vehicle (DMSO) and bleomycin-treated islets at day 4 post-drug removal. Data are means ± SD of n = 3 biological replicates.

C) Luminex assays for indicated SASP factors in the conditioned media from islets treated as in (A) at day 5 post-drug removal. Data are normalized to islet RNA content and are means ± SD of n = 3 biological replicates.

D) Overview of experiment on EndoC-βH5 cells. Cells were treated as indicated and harvested for western blotting, qRT-PCR and Luminex assays.

bioRxiv preprint doi: https://doi.org/10.1101/2021.06.07.447428; this version posted December 22, 2021. The copyright holder for this preprint (which was not certified by peer review) is the author/funder, who has granted bioRxiv a license to display the preprint in perpetuity. It is made available under aCC-BY-NC-ND 4.0 International license.

E) Western blot analysis of DDR and early senescence markers in cells treated as indicated. Data are means ± SD of n = 3 biological replicates.

F) qRT-PCR analysis of senescence genes *CDKN1A, CDKN2A*, prosurvival gene *BCL2L1* (encoding BCL-XL) and SASP gene *CXCL8* (encoding IL-8) in EndoC cells treated as in (A) at day 2 post-drug removal. Data are means ± SD of n = 3 biological replicates.

G) Luminex assays of indicated SASP factors in the conditioned media from EndoC cells treated as in (A) at day 5 post-drug removal. Data are normalized to viable cell counts and are means ± SD of n = 4 biological replicates.

For all panels, *p<0.05, **p<0.005, ***p<0.0005, two-tailed T-tests.

Figure 6. Senescence leads to decreased insulin content.

A) GSIS assays and total insulin content of MIN6 and NIT1 cells treated with vehicle or etoposide at 72 h post-treatment. Data are means ± SD of n = 4 biological replicates.

B) GSIS assays and total insulin content of human islets from a 55 year-old male donor treated with vehicle or bleomycin at day 4 post-drug removal. Data are means ± SD of n = 6 biological replicates.

For GSIS panels, *p<0.05, **p<0.005, ***p<0.0005, Two-way ANOVAs.

For Insulin content panels, *p< 0.05, **p<0.005, two-tailed T-tests.

bioRxiv preprint doi: https://doi.org/10.1101/2021.06.07.447428; this version posted December 22, 2021. The copyright holder for this preprint (which was not certified by peer review) is the author/funder, who has granted bioRxiv a license to display the preprint in perpetuity. It is made available under aCC-BY-NC-ND 4.0 International license.

References

[1] Katsarou, A., Gudbjornsdottir, S., Rawshani, A., Dabelea, D., Bonifacio, E., Anderson, B.J., et al., 2017. Type 1 diabetes mellitus. Nature Reviews. Disease Primers 3: 17016, Doi: 10.1038/nrdp.2017.16.

[2] Eizirik, D.L., Pasquali, L., Cnop, M., 2020. Pancreatic β-cells in type 1 and type 2 diabetes mellitus: different pathways to failure. Nature Reviews Endocrinology 16(7): 349–62, Doi: 10.1038/s41574-020-0355-7.

[3] Roep, B.O., Thomaidou, S., Tienhoven, R. van., Zaldumbide, A., 2020. Type 1 diabetes mellitus as a disease of the β- cell (do not blame the immune system?). Nature Reviews Endocrinology 17(3): 150–61, Doi: 10.1038/s41574-020-00443-4.

[4] Sahin, G.S., Lee, H., Engin, F., 2021. An accomplice more than a mere victim: The impact of β-cell ER stress on type 1 diabetes pathogenesis. Molecular Metabolism: 101365, Doi: https://doi.org/10.1016/j.molmet.2021.101365.

[5] Ovalle, F., Grimes, T., Xu, G., Patel, A.J., Grayson, T.B., Thielen, L.A., et al., 2018. Verapamil and beta cell function in adults with recent-onset type 1 diabetes. Nature Medicine 24(8): 1108–12, Doi: 10.1038/s41591-018-0089-4.

[6] Gitelman, S.E., Bundy, B.N., Ferrannini, E., Lim, N., Blanchfield, J.L., DiMeglio, L.A., et al., 2021. Imatinib therapy for patients with recent-onset type 1 diabetes: a multicentre, randomised, double-blind, placebo-controlled, phase 2 trial. The Lancet Diabetes and Endocrinology 9(8): 502–14, Doi: 10.1016/S2213-8587(21)00139-X.

bioRxiv preprint doi: https://doi.org/10.1101/2021.06.07.447428; this version posted December 22, 2021. The copyright holder for this preprint (which was not certified by peer review) is the author/funder, who has granted bioRxiv a license to display the preprint in perpetuity. It is made available under aCC-BY-NC-ND 4.0 International license.

[7] Thompson, P.J., Shah, A., Ntranos, V., Van Gool, F., Atkinson, M., Bhushan, A., 2019. Targeted Elimination of Senescent Beta Cells Prevents Type 1 Diabetes. Cell Metabolism 29(5): 1045–60, Doi: 10.1016/j.cmet.2019.01.021.

[8] He, S., Sharpless, N.E., 2017. Senescence in Health and Disease. Cell 169(6): 1000–11, Doi: 10.1016/j.cell.2017.05.015.

[9] Herranz, N., Gil, J., 2018. Mechanisms and functions of cellular senescence. Journal of Clinical Investigation 128(4): 1238–46, Doi: 10.1172/JCI95148.

[10] Childs, B.G., Gluscevic, M., Baker, D.J., Laberge, R.M., Marquess, D., Dananberg, J., et al., 2017. Senescent cells: An emerging target for diseases of ageing. Nature Reviews Drug Discovery 16(10): 718–35, Doi: 10.1038/nrd.2017.116.

[11] Helman, A., Avrahami, D., Klochendler, A., Glaser, B., Kaestner, K.H., Ben-Porath, I., et al., 2016. Effects of ageing and senescence on pancreatic β-cell function. Diabetes, Obesity and Metabolism 18(September): 58–62, Doi: 10.1111/dom.12719.

[12] Brawerman, G., Thompson, P.J., 2020. Beta cell therapies for preventing type 1 diabetes: From bench to bedside. Biomolecules 10(12): 1–20, Doi: 10.3390/biom10121681.

[13] Aguayo-Mazzucato, C., Andle, J., Lee, T.B., Midha, A., Talemal, L., Chipashvili, V., et al., 2019. Acceleration of β Cell Aging Determines Diabetes and Senolysis Improves Disease Outcomes. Cell Metabolism 30(1): 129-142.e4, Doi: 10.1016/j.cmet.2019.05.006.

[14] Thompson, P.J., Shah, A., Apostolopolou, H., Bhushan, A., 2019. BET proteins are required for transcriptional activation of the senescent islet cell secretome in type 1 diabetes. International Journal of Molecular Sciences 20(19): 1–13, Doi: 10.3390/ijms20194776.

[15] Hernandez-Segura, A., de Jong, T. V., Melov, S., Guryev, V., Campisi, J., Demaria, M., 2017. Unmasking Transcriptional Heterogeneity in Senescent Cells. Current Biology 27(17): 2652-2660.e4, Doi: 10.1016/j.cub.2017.07.033.

[16] Wiley, C.D., Flynn, J.M., Morrissey, C., Lebofsky, R., Shuga, J., Dong, X., et al., 2017. Analysis of individual cells identifies cell-to-cell variability following induction of cellular senescence. Aging Cell 16(5): 1043–50, Doi: 10.1111/acel.12632.

[17] Sharpless, N.E., Sherr, C.J., 2015. Forging a signature of in vivo senescence. Nature Reviews Cancer 15(7): 397–408, Doi: 10.1038/nrc3960.

[18] Dooley, J., Tian, L., Schonefeldt, S., Delghingaro-Augusto, V., Garcia-Perez, J.E., Pasciuto, E., et al., 2016. Genetic predisposition for beta cell fragility underlies type 1 and type 2 diabetes. Nature Genetics 48(5): 519–27, Doi: 10.1038/ng.3531.

[19] Horwitz, E., Krogvold, L., Zhitomirsky, S., Swisa, A., Fischman, M., Lax, T., et al., 2018. Beta Cell DNA Damage Response Promotes Islet Inflammation in Type 1

bioRxiv preprint doi: https://doi.org/10.1101/2021.06.07.447428; this version posted December 22, 2021. The copyright holder for this preprint (which was not certified by peer review) is the author/funder, who has granted bioRxiv a license to display the preprint in perpetuity. It is made available under aCC-BY-NC-ND 4.0 International license.

Diabetes. Diabetes 67(11): 2305–11, Doi: 10.2337/db17-1006.

[20] Miyazaki, J.I., Araki, K., Yamato, E., Ikegami, H., Asano, T., Shibasaki, Y., et al., 1990. Establishment of a pancreatic β cell line that retains glucose-inducible insulin secretion: Special reference to expression of glucose transporter isoforms. Endocrinology 127(1): 126–32, Doi: 10.1210/endo-127-1-126.

[21] Hamaguchi, K., Gaskins, H.R., Leiter, E.H., 1991. NIT-1, a pancreatic β-cell line established from a transgenic NOD/Lt mouse. Diabetes 40(7): 842–9, Doi: 10.2337/diab.40.7.842.

[22] Flor, A.C., Wolfgeher, D., Wu, D., Kron, S.J., 2017. A signature of enhanced lipid metabolism, lipid peroxidation and aldehyde stress in therapy-induced senescence. Cell Death Discovery 3(1): 1–12, Doi: 10.1038/cddiscovery.2017.75.

[23] Scharfmann, R., Staels, W., Albagli, O., 2019. The supply chain of human pancreatic β cell lines. Journal of Clinical Investigation 129(9): 3511–20, Doi: 10.1172/JCI129484.

[24] Benazra, M., Lecomte, M.-J., Colace, C., Müller, A., Machado, C., Pechberty, S., et al., 2015. A human beta cell line with drug inducible excision of immortalizing transgenes. Molecular Metabolism 4(12): 916–25, Doi: 10.1016/j.molmet.2015.09.008.

[25] Martin, M., 2011. Cutadapt removes adapter sequences from high-throughput sequencing reads. Embnet Journal 17(1): 10–2.

[26] Langmead, B., Salzberg, S.L., 2012. Fast gapped-read alignment with Bowtie 2. Nature Methods 9(4): 357–9, Doi: 10.1038/nmeth.1923.

[27] Kim, D., Langmead, B., Salzberg, S.L., 2015. HISAT: a fast spliced aligner with low memory requirements. Nature Methods 12(4): 357–60, Doi: 10.1038/nmeth.3317.

[28] Pertea, M., Pertea, G.M., Antonescu, C.M., Chang, T.-C., Mendell, J.T., Salzberg, S.L., 2015. StringTie enables improved reconstruction of a transcriptome from RNA-seq reads. Nature Biotechnology 33(3): 290–5, Doi: 10.1038/nbt.3122.

[29] Robinson, M.D., McCarthy, D.J., Smyth, G.K., 2010. edgeR: a Bioconductor package for differential expression analysis of digital gene expression data. Bioinformatics (Oxford, England) 26(1): 139–40, Doi: 10.1093/bioinformatics/btp616.

[30] Kong, L., Zhang, Y., Ye, Z.-Q., Liu, X.-Q., Zhao, S.-Q., Wei, L., et al., 2007. CPC: assess the protein-coding potential of transcripts using sequence features and support vector machine. Nucleic Acids Research 35(Web Server issue): W345-9, Doi: 10.1093/nar/gkm391.

[31] Sun, L., Luo, H., Bu, D., Zhao, G., Yu, K., Zhang, C., et al., 2013. Utilizing sequence intrinsic composition to classify protein-coding and long non-coding transcripts. Nucleic Acids Research 41(17): e166, Doi: 10.1093/nar/gkt646.

bioRxiv preprint doi: https://doi.org/10.1101/2021.06.07.447428; this version posted December 22, 2021. The copyright holder for this preprint (which was not certified by peer review) is the author/funder, who has granted bioRxiv a license to display the preprint in perpetuity. It is made available under aCC-BY-NC-ND 4.0 International license.

[32] Seshadri, N., Jonasson, M.E., Hunt, K.L., Xiang, B., Cooper, S., Wheeler, M.B., et al., 2017. Uncoupling protein 2 regulates daily rhythms of insulin secretion capacity in MIN6 cells and isolated islets from male mice. Molecular Metabolism 6(7): 760–9, Doi: 10.1016/j.molmet.2017.04.008.

[33] Lyon, J., Manning Fox, J.E., Spigelman, A.F., Kim, R., Smith, N., O'Gorman, D., et al., 2016. Research-Focused Isolation of Human Islets From Donors With and Without Diabetes at the Alberta Diabetes Institute IsletCore. Endocrinology 157(2): 560–9, Doi: 10.1210/en.2015-1562.

[34] Midha, A., Pan, H., Abarca, C., Andle, J., Carapeto, P., Bonner-Weir, S., et al., 2021. Unique human and mouse β-cell senescence-associated secretory phenotype (SASP) reveal conserved signaling pathways and heterogeneous factors. Diabetes 70(5): 1098–116, Doi: 10.2337/db20-0553.

[35] Froelich-Ammon, S.J., Osheroff, N., 1995. Topoisomerase poisons: Harnessing the dark side of enzyme mechanism. Journal of Biological Chemistry 270(37): 21429–32, Doi: 10.1074/jbc.270.37.21429.

[36] Brown, E., Watkin, D., Evans, J., Yip, V., Cuthbertson, D.J., 2018. Multidisciplinary management of refractory insulinomas. Clinical Endocrinology 88(5): 615–24, Doi: 10.1111/cen.13528.

[37] Tavana, O., Puebla-osorio, N., Sang, M., Zhu, C., 2010. Nonhomologous End-Joining Deficiency Leads to a Severe Diabetic Phenotype in Mice. Diabetes 59(January), Doi: 10.2337/db09-0792.O.T.

[38] Chesnokova, V., Wong, C., Zonis, S., Gruszka, A., Wawrowsky, K., 2009. Diminished pancreatic beta-cell mass in securin-null mice is caused by beta-cell apoptosis and senescence. Endocrinology 150(June 2009): 2603–10, Doi: 10.1210/en.2008-0972.

[39] Basisty, N., Kale, A., Jeon, O.H., Kuehnemann, C., Payne, T., Rao, C., et al., 2020. A Proteomic Atlas of Senescence-Associated Secretomes for Aging Biomarker Development. PLoS Biology 18(1): e3000599, Doi: https://doi.org/10.1371/journal.pbio.3000599.

[40] Paez-Ribes, M., González-Gualda, E., Doherty, G.J., Muñoz-Espín, D., 2019. Targeting senescent cells in translational medicine. EMBO Molecular Medicine 11(12): 1–19, Doi: 10.15252/emmm.201810234.

[41] Prata, L.G.P.L., Ovsyannikova, I.G., Tchkonia, T., Kirkland, J.L., 2018. Senescent cell clearance by the immune system: Emerging therapeutic opportunities. Seminars in Immunology 40(July 2018): 101275, Doi: 10.1016/j.smim.2019.04.003.

[42] Fischer, M., 2017. Census and evaluation of p53 target genes. Oncogene 36(28): 3943–56, Doi: 10.1038/onc.2016.502.

[43] Freund, A., Laberge, R.-M., Demaria, M., Campisi, J., 2012. Lamin B1 loss is a senescence-associated biomarker. Molecular Biology of the Cell 23(11): 2066–75,

bioRxiv preprint doi: https://doi.org/10.1101/2021.06.07.447428; this version posted December 22, 2021. The copyright holder for this preprint (which was not certified by peer review) is the author/funder, who has granted bioRxiv a license to display the preprint in perpetuity. It is made available under aCC-BY-NC-ND 4.0 International license.

Doi: 10.1091/mbc.E11-10-0884.

[44] Aird, K.M., Iwasaki, O., Kossenkov, A. V., Tanizawa, H., Fatkhutdinov, N., Bitler, B.G., et al., 2016. HMGB2 orchestrates the chromatin landscape of senescence-associated secretory phenotype gene loci. Journal of Cell Biology 215(3): 325–34, Doi: 10.1083/jcb.201608026.

[45] Liu, F.J., Wen, T., Liu, L., 2012. MicroRNAs as a novel cellular senescence regulator. Ageing Research Reviews 11(1): 41–50, Doi: 10.1016/j.arr.2011.06.001.

[46] Schmitt, A.M., Garcia, J.T., Hung, T., Flynn, R.A., Shen, Y., Qu, K., et al., 2016. An inducible long noncoding RNA amplifies DNA damage signaling. Nature Genetics 48(11): 1370–6, Doi: 10.1038/ng.3673.

[47] Chen, Y.C., Taylor, A.J., Verchere, C.B., 2018. Islet prohormone processing in health and disease. Diabetes, Obesity and Metabolism 20(May): 64–76, Doi: 10.1111/dom.13401.

[48] Seiron, P., Stenwall, A., Hedin, A., Granlund, L., Esguerra, J.L.S., Volkov, P., et al., 2021. Transcriptional analysis of islets of Langerhans from organ donors of different ages. PLoS ONE 16(3 March): 1–13, Doi: 10.1371/journal.pone.0247888.

[49] Colli, M.L., Ramos-Rodríguez, M., Nakayasu, E.S., Alvelos, M.I., Lopes, M., Hill, J.L.E., et al., 2020. An integrated multi-omics approach identifies the landscape of interferon-α-mediated responses of human pancreatic beta cells. Nature Communications 11(1), Doi: 10.1038/s41467-020-16327-0.

[50] Novakova, Z., Hubackova, S., Kosar, M., Janderova-Rossmeislova, L., Dobrovolna, J., Vasicova, P., et al., 2010. Cytokine expression and signaling in drug-induced cellular senescence. Oncogene 29(2): 273–84, Doi: 10.1038/onc.2009.318.

[51] Irvine, K.M., Skoien, R., Bokil, N.J., Melino, M., Thomas, G.P., Loo, D., et al., 2014. Senescent human hepatocytes express a unique secretory phenotype and promote macrophage migration. World Journal of Gastroenterology 20(47): 17851–62, Doi: 10.3748/wjg.v20.i47.17851.

[52] Steiner, D.J., Kim, A., Miller, K., Hara, M., 2010. Pancreatic islet plasticity: Interspecies comparison of islet architecture and composition. Islets 2(3), Doi: 10.4161/isl.2.3.11815.

[53] Colli, M.L., Ramos-Rodríguez, M., Nakayasu, E.S., Alvelos, M.I., Lopes, M., Hill, J.L.E., et al., 2020. An integrated multi-omics approach identifies the landscape of interferon-α-mediated responses of human pancreatic beta cells. Nature Communications 11(1), Doi: 10.1038/s41467-020-16327-0.

[54] Helman, A., Klochendler, A., Azazmeh, N., Gabai, Y., Horwitz, E., Anzi, S., et al., 2016. p16(Ink4a)-induced senescence of pancreatic beta cells enhances insulin secretion. Nature Medicine 22(4): 412–20, Doi: 10.1038/nm.4054.

bioRxiv preprint doi: https://doi.org/10.1101/2021.06.07.447428; this version posted December 22, 2021. The copyright holder for this preprint (which was not certified by peer review) is the author/funder, who has granted bioRxiv a license to display the preprint in perpetuity. It is made available under aCC-BY-NC-ND 4.0 International license.

[55] Köhler, C.U., Olewinski, M., Tannapfel, A., Schmidt, W.E., Fritsch, H., Meier, J.J., 2011. Cell cycle control of β-cell replication in the prenatal and postnatal human pancreas. American Journal of Physiology - Endocrinology and Metabolism 300(1), Doi: 10.1152/ajpendo.00496.2010.

[56] Zhu, Y., Tchkonia, T., Pirtskhalava, T., Gower, A.C., Ding, H., Giorgadze, N., et al., 2015. The Achilles' heel of senescent cells: From transcriptome to senolytic drugs. Aging Cell (March): 644–58, Doi: 10.1111/acel.12344.

[57] Yosef, R., Pilpel, N., Tokarsky-Amiel, R., Biran, A., Ovadya, Y., Cohen, S., et al., 2016. Directed elimination of senescent cells by inhibition of BCL-W and BCL-XL. Nature Communications 7: 11190, Doi: 10.1038/ncomms11190.

[58] Hoare, M., Ito, Y., Kang, T.-W., Weekes, M.P., Matheson, N.J., Patten, D.A., et al., 2016. NOTCH1 mediates a switch between two distinct secretomes during senescence. Nature Cell Biology 18(9): 979–92, Doi: 10.1038/ncb3397.

[59] Nakayasu, E.S., Syed, F., Tersey, S.A., Gritsenko, M.A., Mitchell, H.D., Chan, C.Y., et al., 2020. Comprehensive Proteomics Analysis of Stressed Human Islets Identifies GDF15 as a Target for Type 1 Diabetes Intervention. Cell Metabolism 31(2): 363-374.e6, Doi: 10.1016/j.cmet.2019.12.005.

[60] Ward-Kavanagh, L.K., Lin, W.W., Šedý, J.R., Ware, C.F., 2016. The TNF Receptor Superfamily in Co-stimulating and Co-inhibitory Responses. Immunity 44(5): 1005–19, Doi: 10.1016/j.immuni.2016.04.019.

[61] Palmer, A.K., Xu, M., Zhu, Y., Pirtskhalava, T., Weivoda, M.M., Hachfeld, C.M., et al., 2019. Targeting senescent cells alleviates obesity-induced metabolic dysfunction. Aging Cell 18(3): 1–15, Doi: 10.1111/acel.12950.

[62] Pearson, G.L., Gingerich, M.A., Walker, E.M., Biden, T.J., Soleimanpour, S.A., 2021. A Selective Look at Autophagy in Pancreatic β-Cells. Diabetes 70(6): 1229–41, Doi: 10.2337/dbi20-0014.

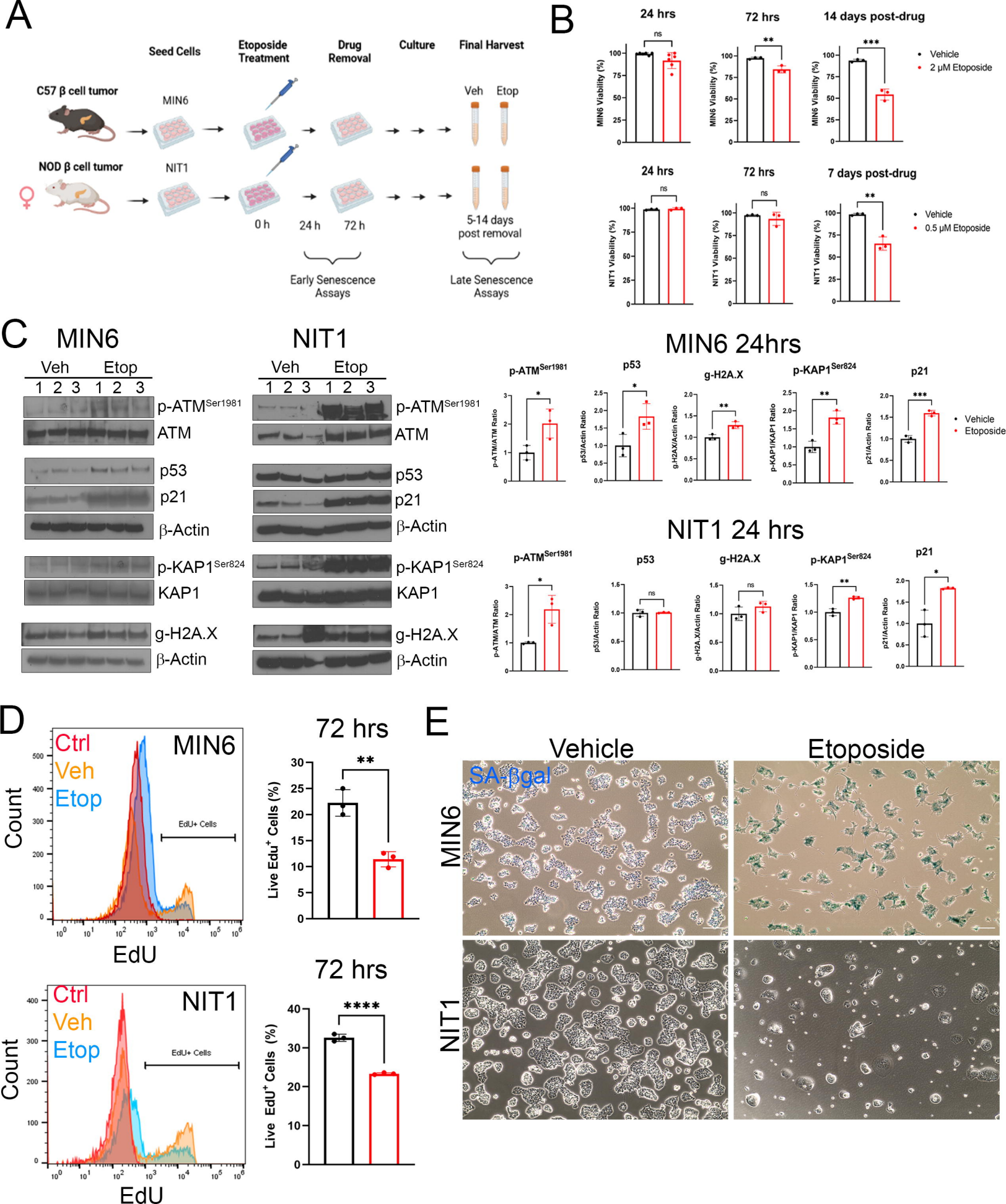
A
Seed Cells
Etoposide Treatment
Drug Removal
Culture
Final Harvest
C57 β cell tumor
MIN6
Veh
Etop
NOD β cell tumor
NIT1
0 h
24 h
72 h
5-14 days post removal
Early Senescence Assays
Late Senescence Assays
B
24 hrs
72 hrs
14 days post-drug
MIN6 Viability (%)
Vehicle
2 μM Etoposide
7 days post-drug
NIT1 Viability (%)
0.5 μM Etoposide
C
MIN6
NIT1
Veh
Etop
p-ATM Ser1981
ATM
p53
p21
β-Actin
p-KAP1 Ser824
KAP1
g-H2A.X
MIN6 24hrs
NIT1 24 hrs
p-ATM/ATM Ratio
p53/Actin Ratio
g-H2AX/Actin Ratio
p-KAP1/KAP1 Ratio
p21/Actin Ratio
Vehicle
Etoposide
D
Ctrl
Veh
Etop
MIN6
NIT1
EdU+ Cells
Count
EdU
72 hrs
Live EdU+ Cells (%)
E
Vehicle
Etoposide
SA-βgal
MIN6
NIT1

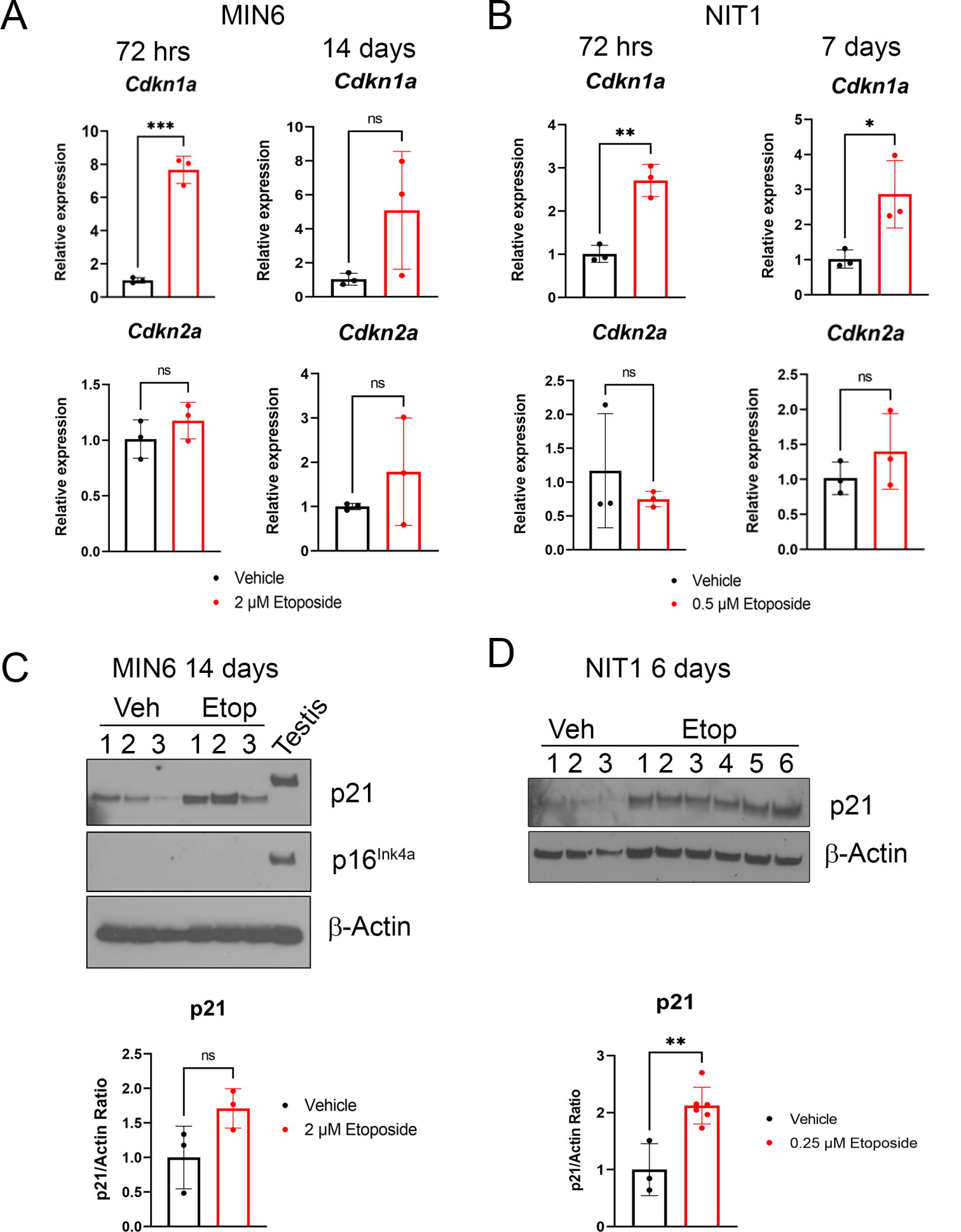
A
MIN6
72 hrs
14 days
Cdkn1a
Cdkn2a
Relative expression
***
ns
Vehicle
2 μM Etoposide
B
NIT1
72 hrs
7 days
**
*
0.5 μM Etoposide
C
MIN6 14 days
Veh
Etop
1 2 3 1 2 3
Testis
p21
p16Ink4a
β-Actin
p21/Actin Ratio
D
NIT1 6 days
1 2 3 1 2 3 4 5 6
0.25 μM Etoposide

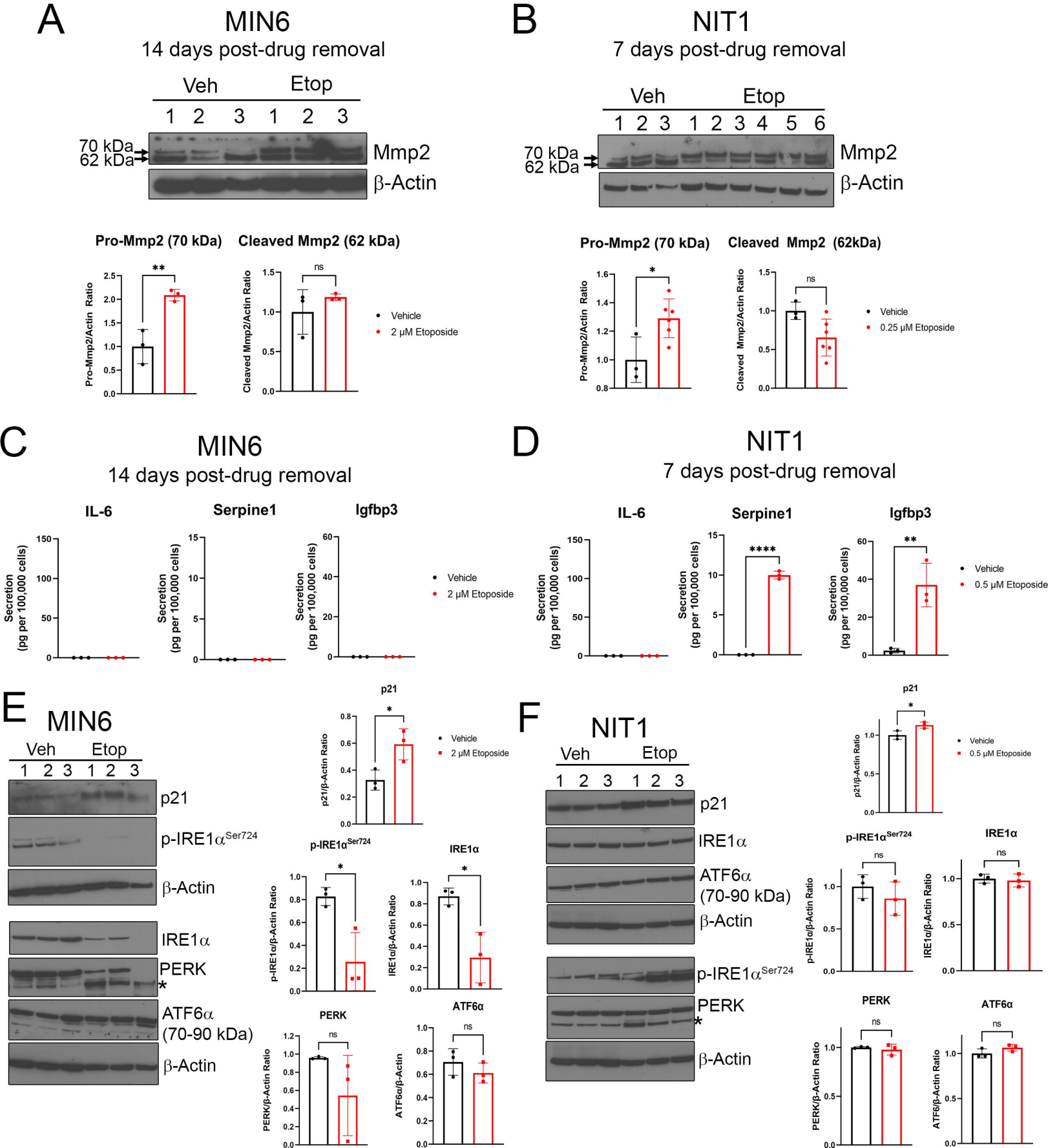
A
MIN6
14 days post-drug removal
Veh
Etop
1 2 3 1 2 3
70 kDa
62 kDa
Mmp2
β-Actin
Pro-Mmp2 (70 kDa)
Cleaved Mmp2 (62 kDa)
Pro-Mmp2/Actin Ratio
Cleaved Mmp2/Actin Ratio
**
ns
Vehicle
2 μM Etoposide
B
NIT1
7 days post-drug removal
Veh
Etop
1 2 3 1 2 3 4 5 6
70 kDa
62 kDa
Mmp2
β-Actin
Pro-Mmp2 (70 kDa)
Cleaved Mmp2 (62kDa)
Pro-Mmp2/Actin Ratio
Cleaved Mmp2/Actin Ratio
*
ns
Vehicle
0.25 μM Etoposide
C
MIN6
14 days post-drug removal
IL-6
Serpine1
Igfbp3
Secretion (pg per 100,000 cells)
Vehicle
2 μM Etoposide
D
NIT1
7 days post-drug removal
IL-6
Serpine1
Igfbp3
Secretion (pg per 100,000 cells)
****
**
Vehicle
0.5 μM Etoposide
E
MIN6
Veh
Etop
1 2 3 1 2 3
p21
p-IRE1α Ser724
β-Actin
IRE1α
PERK
*
ATF6α (70-90 kDa)
β-Actin
p21
p21/β-Actin Ratio
*
Vehicle
2 μM Etoposide
p-IRE1α Ser724
IRE1α
p-IRE1α/β-Actin Ratio
IRE1α/β-Actin Ratio
PERK
ATF6α
PERK/β-Actin Ratio
ATF6α/β-Actin
ns
F
NIT1
Veh
Etop
1 2 3 1 2 3
p21
IRE1α
ATF6α (70-90 kDa)
β-Actin
p-IRE1α Ser724
PERK
*
β-Actin
p21
p21/β-Actin Ratio
*
Vehicle
0.5 μM Etoposide
p-IRE1α Ser724
IRE1α
p-IRE1α/β-Actin Ratio
IRE1α/β-Actin Ratio
PERK
ATF6α
PERK/β-Actin Ratio
ATF6/β-Actin Ratio
ns

bioRxiv preprint doi: https://doi.org/10.1101/2021.06.07.447428; this version posted December 22, 2021. The copyright holder for this preprint (which was not certified by peer review) is the author/funder, who has granted bioRxiv a license to display the preprint in perpetuity. It is made available under aCC-BY-NC-ND 4.0 International license.

A

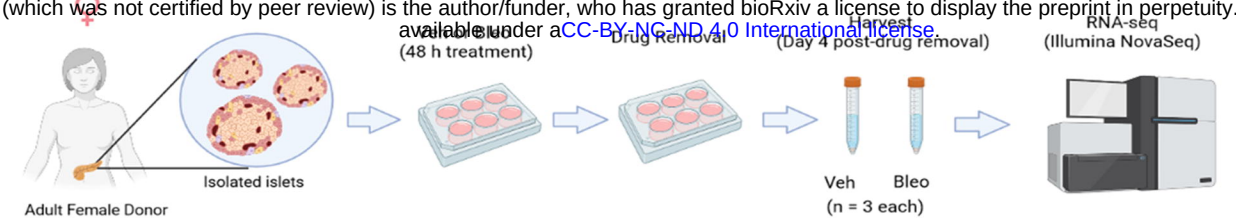

B

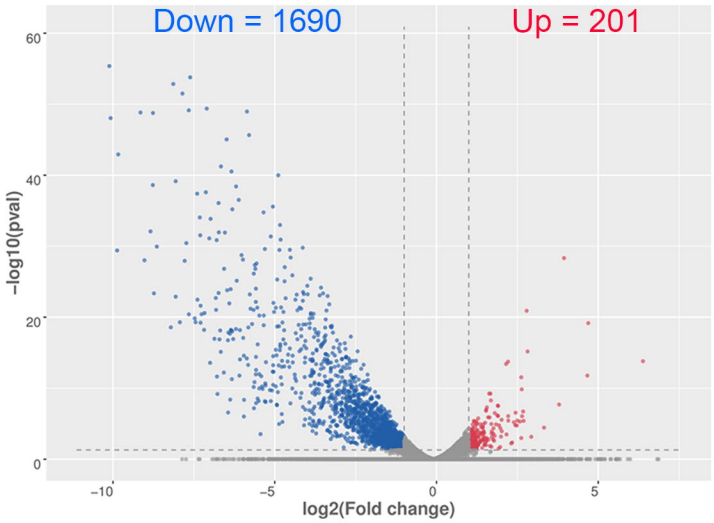

C

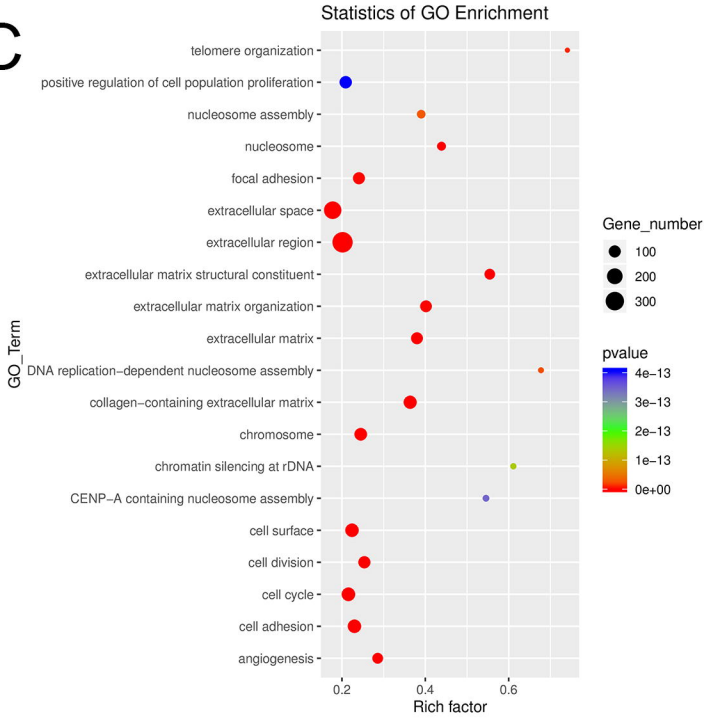

D

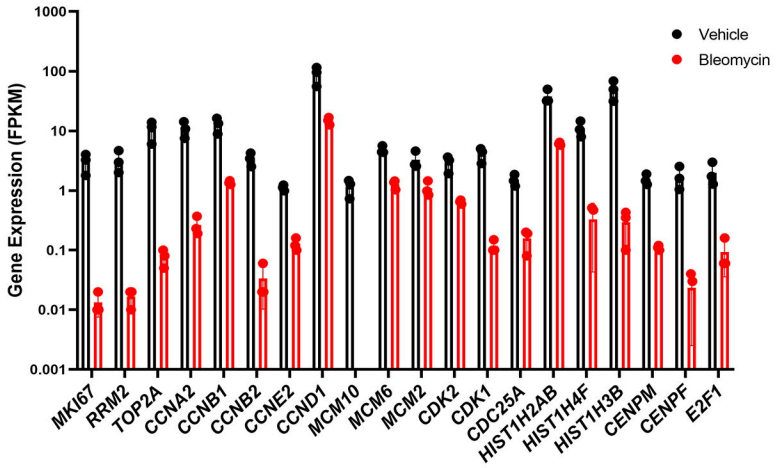

E

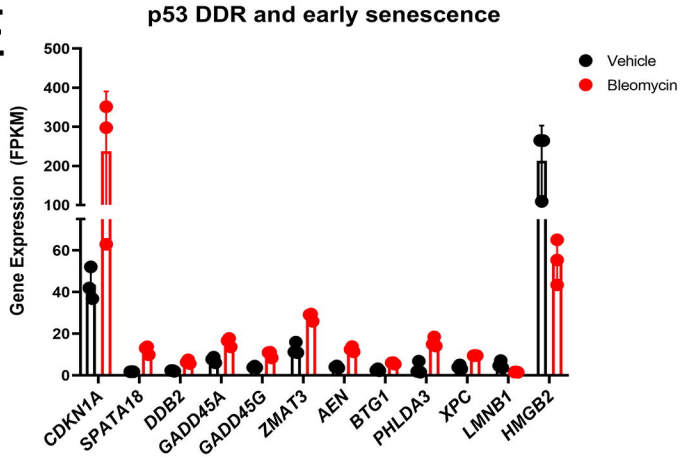

F

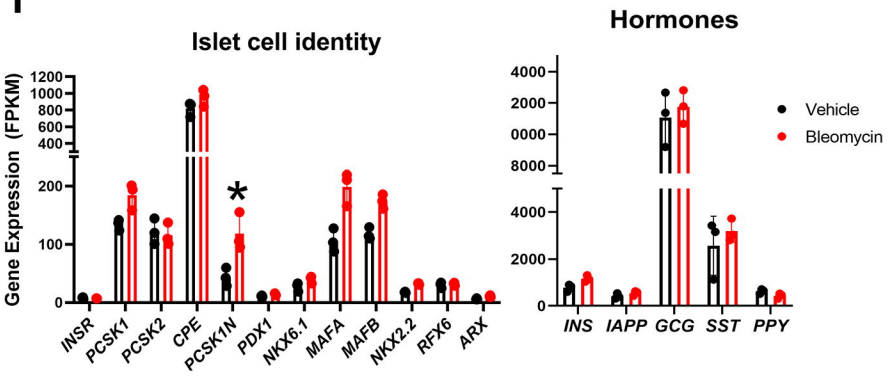

G

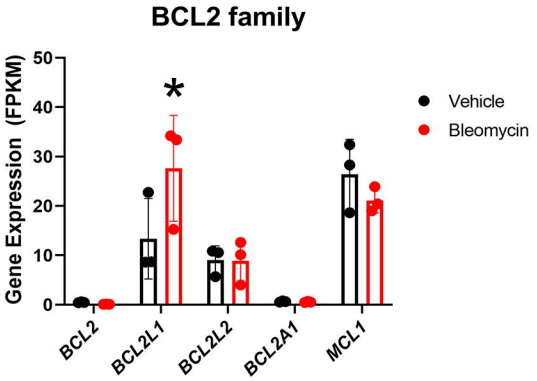

H

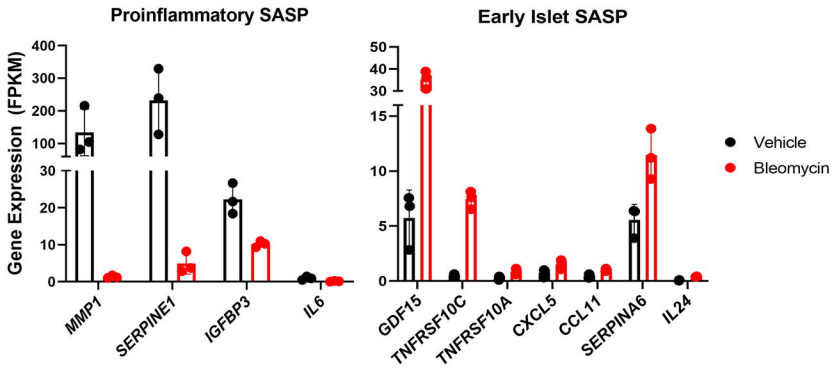

bioRxiv preprint doi: https://doi.org/10.1101/2021.06.07.447428; this version posted December 22, 2021. The copyright holder for this preprint (which was not certified by peer review) is the author/funder, who has granted bioRxiv a license to display the preprint in perpetuity. It is made available under a CC-BY-NC-ND 4.0 International license.

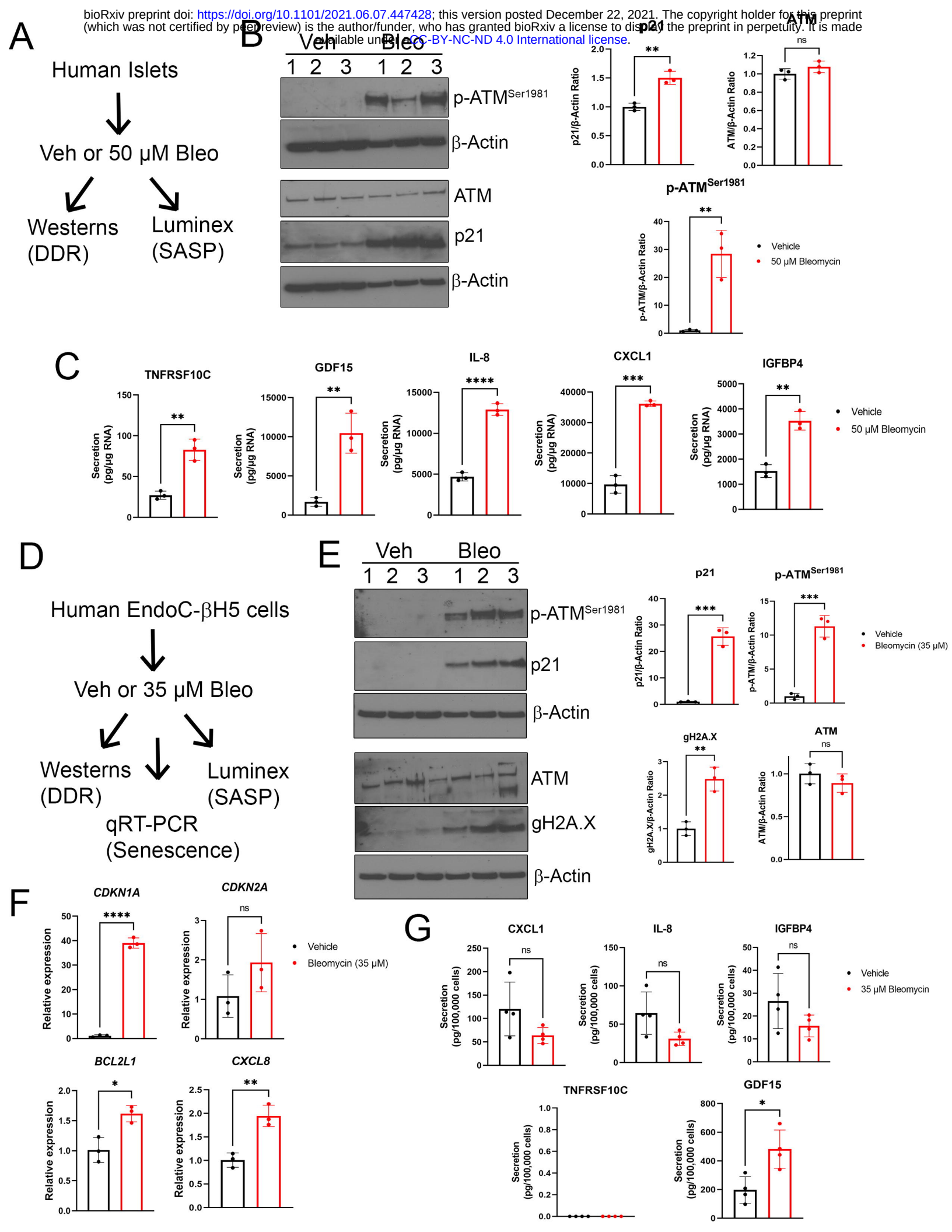

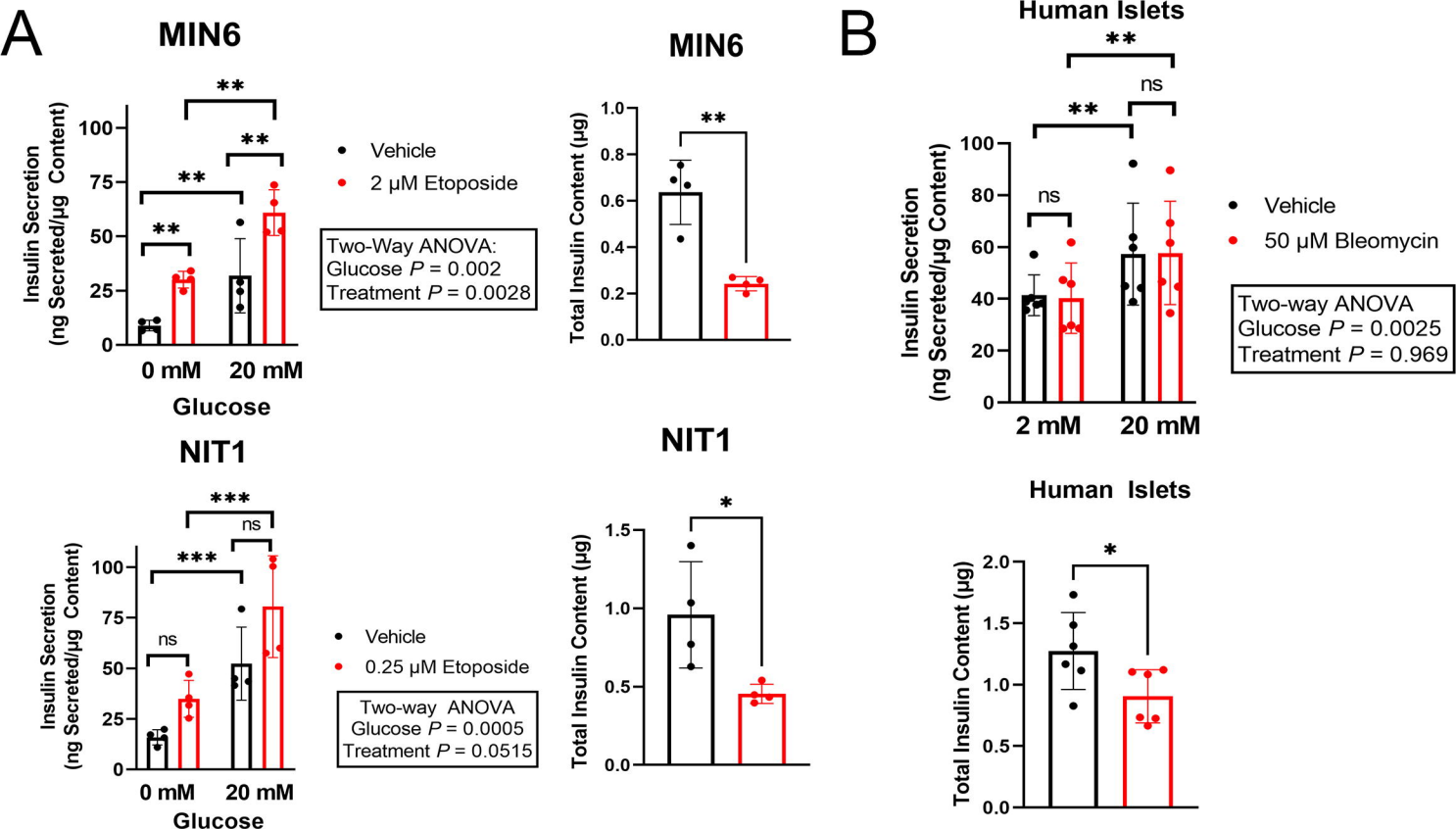
A
MIN6
Insulin Secretion (ng Secreted/µg Content)
100
75
50
25
0
**
**
**
**
0 mM
20 mM
Glucose
Vehicle
2 µM Etoposide
Two-Way ANOVA:
Glucose P = 0.002
Treatment P = 0.0028
MIN6
Total Insulin Content (µg)
1.0
0.8
0.6
0.4
0.2
0.0
**
NIT1
Insulin Secretion (ng Secreted/µg Content)
100
75
50
25
0
***
***
ns
ns
0 mM
20 mM
Glucose
Vehicle
0.25 µM Etoposide
Two-way ANOVA
Glucose P = 0.0005
Treatment P = 0.0515
NIT1
Total Insulin Content (µg)
1.5
1.0
0.5
0.0
*
B
Human Islets
Insulin Secretion (ng Secreted/µg Content)
100
80
60
40
20
0
**
**
ns
ns
2 mM
20 mM
Vehicle
50 µM Bleomycin
Two-way ANOVA
Glucose P = 0.0025
Treatment P = 0.969
Human Islets
Total Insulin Content (µg)
2.0
1.5
1.0
0.5
0.0
*